

# Journal Pre-proof

Design and synthesis of 1*H*-indazole-3-carboxamide derivatives as potent and selective PAK1 inhibitors with anti-tumour migration and invasion activities

Mingliang Zhang, Xiaobao Fang, Cong Wang, Chen Huang, Meng Wang, Lu Zhu, Zixu Wang, Yuhan Gao, Tianyi Zhang, Haichun Liu, Yanmin Zhang, Shuai Lu, Tao Lu, Yadong Chen, Hongmei Li

PII: S0223-5234(20)30489-X

DOI: <https://doi.org/10.1016/j.ejmech.2020.112517>

Reference: EJMECH 112517

To appear in: *European Journal of Medicinal Chemistry*

Received Date: 6 January 2020

Revised Date: 15 May 2020

Accepted Date: 29 May 2020

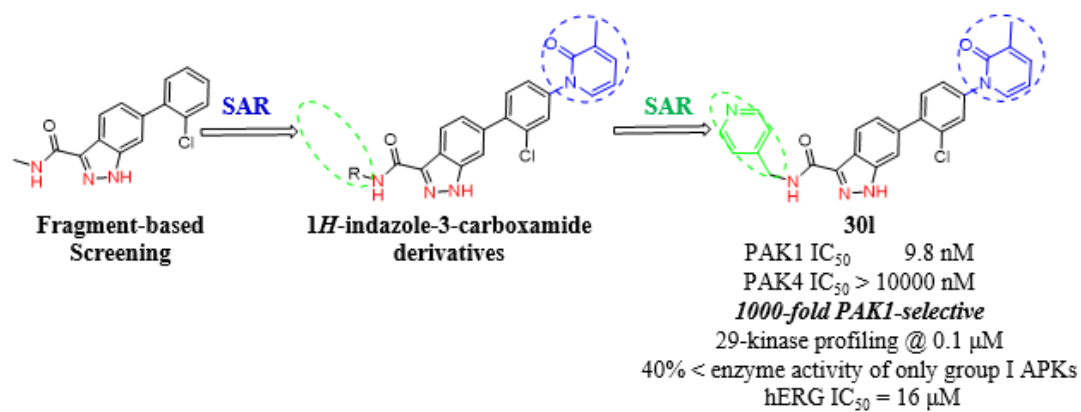
Please cite this article as: M. Zhang, X. Fang, C. Wang, C. Huang, M. Wang, L. Zhu, Z. Wang, Y. Gao, T. Zhang, H. Liu, Y. Zhang, S. Lu, T. Lu, Y. Chen, H. Li, Design and synthesis of 1*H*-indazole-3-carboxamide derivatives as potent and selective PAK1 inhibitors with anti-tumour migration and invasion activities, *European Journal of Medicinal Chemistry*, <https://doi.org/10.1016/j.ejmech.2020.112517>.

This is a PDF file of an article that has undergone enhancements after acceptance, such as the addition of a cover page and metadata, and formatting for readability, but it is not yet the definitive version of record. This version will undergo additional copyediting, typesetting and review before it is published in its final form, but we are providing this version to give early visibility of the article. Please note that, during the production process, errors may be discovered which could affect the content, and all legal disclaimers that apply to the journal pertain.

© 2020 Elsevier Masson SAS. All rights reserved.



## Graphical Abstract



## Design and synthesis of 1*H*-indazole-3-carboxamide derivatives as potent and selective PAK1 inhibitors with anti-tumour migration and invasion activities

Mingliang Zhang<sup>a</sup>, Xiaobao Fang<sup>a</sup>, Cong Wang<sup>a</sup>, Chen Huang<sup>a</sup>, Meng Wang<sup>a</sup>, Lu Zhu<sup>a</sup>, Zixu Wang<sup>a</sup>, Yuhan Gao<sup>a</sup>, Tianyi Zhang<sup>a</sup>, Haichun Liu<sup>a</sup>, Yanmin Zhang<sup>a</sup>, Shuai Lu<sup>a</sup>, Tao Lu<sup>a,b\*</sup>, Yadong Chen<sup>a,b\*</sup>, Hongmei Li<sup>a\*</sup>

<sup>a</sup> Laboratory of Molecular Design and Drug Discovery, China Pharmaceutical University, Nanjing 211198, P.R. China.

<sup>b</sup> State Key Laboratory of Natural Medicines, China Pharmaceutical University, Nanjing 210009, P.R. China

### Abstract

Aberrant activation of p21-activated kinase 1 (PAK1) is associated with tumour progression, and PAK1 has been recognized as a promising target for anticancer drug discovery. However, the development of potent PAK1 inhibitors with satisfactory kinase selectivity and favourable physicochemical properties remains a daunting challenge. Herein, we identified the 1*H*-indazole-3-carboxamide derivatives as potential PAK1 inhibitors using a fragment-based screening approach. The representative compound **301** exhibited excellent enzyme inhibition (PAK1 IC<sub>50</sub> = 9.8 nM) and high PAK1 selectivity toward a panel of 29 kinases. The Structure-activity relationship (SAR) analysis showed that substituting of an appropriate hydrophobic ring in the deep back pocket and introducing a hydrophilic group in the bulk solvent region were critical for PAK1 inhibitory activity and selectivity. Additionally, the hERG channel activity of **301** demonstrated its low risk of hERG toxicity. Furthermore, it significantly suppressed the migration and invasion of MDA-MB-231 cells by downregulating Snail expression without affecting the tumour growth. These results provide a new type of chemical scaffolds targeting PAK1 and suggested that 1*H*-indazole-3-carboxamide derivatives may serve as lead compounds for the development of potential and selective PAK1 inhibitors.

**Keywords:** PAK1 inhibitor, kinase selectivity, 1*H*-indazole-3-carboxamide scaffold, anti-tumour metastasis

## 1. Introduction

The p21-activated kinases (PAKs) are Ser/Thr kinases in the STE20 kinase family that function as downstream signalling effectors of the Rho/Rac family of GTPases [1-3]. This family consists of six subtypes and is subdivided into two groups based on their structural homology and regulatory functional characteristics: group I, including PAK1, PAK2 and PAK3, and group II, including PAK4, PAK5 and PAK6. Although these kinases show a high level of structural homology, their tissue expression, subcellular localization, activation mechanism and downstream substrate specificity are not consistent in various physiological processes. As key components of the Rho family, PAKs govern many fundamental cellular processes, including cytoskeletal remodelling, morphological variation and cell migration during cancer progression [4].

Among the group I PAK family, PAK1 has been implicated in multiple oncogenic signalling pathways and is frequently overexpressed in malignancies such as breast, colon and bladder cancers, leading to the poor prognosis [5-7]. Phosphorylation and subsequent activation of PAK1 regulate the PI3K/Akt and Raf/MEK/ERK pathways [8, 9], which transduces the signal downstream and thus contributes to tumour progression. Importantly, increased expression and/or activation of PAK1 induce the epithelial-mesenchymal transition (EMT) by activating the zinc transcription factor [10, 11]. PAK1 predominantly promotes the transcriptional repression activity of Snail from E-cadherin promoters and results in cancer metastasis [12]. Therefore, PAK1 has emerged as a promising target for cancer therapeutics due to its liaison roles in tumor malignancy [13, 14].

Researchers have expressed considerable interest in the development of small-molecule inhibitors targeting PAK1 in recent years (**Fig. 1**). PF-3578309 (**1**), a pan-PAK inhibitor, was the first compound advanced to phase I trials (NCT00932126), but was not progressed due to undesirable pharmacokinetic characteristics and adverse events [15]. Compound **2** and compound **3** (FRAX1036) containing aminopyrazole or pyrido[2,3-d]pyrimidine-7-one scaffolds, respectively, displayed potential as group I PAK-selective inhibitors with exquisite kinase selectivity (more than 100-fold) [3, 16]. Since selective inhibitors of PAK1 might exert advantageous effects compared with pan inhibitors from a certain medicinal perspective, these compounds have been used as probe compounds to evaluate group I PAK biology [17-19]. Nevertheless, the poor anti-tumour effectiveness at the cellular level has restrained the extensive application of these inhibitors [17]. Recently, Genentech

modified the pyrido[2,3-d]pyrimidine-7-one scaffold by introducing basic amine group to obtain the compounds G5555 (**4**) [20] and G9791 (**5**) [21], which showed high PAK1 selectivity and satisfactory cellular potency. However, their pharmacokinetics and anti-tumour efficiency *in vivo* have not yet been disclosed. With the exception of the aminopyrazole and pyrido[2,3-d]pyrimidine-7-one scaffolds, other chemotypes have rarely been reported. The similar sequences between PAK isoforms also prevent the development of a PAK1-selective inhibitor that does not block PAK4 activity. Thus, the discovery of alternative chemotypes of potent and highly selective inhibitors are urgently needed to exploit the functions of PAK1 and treat its related disease.

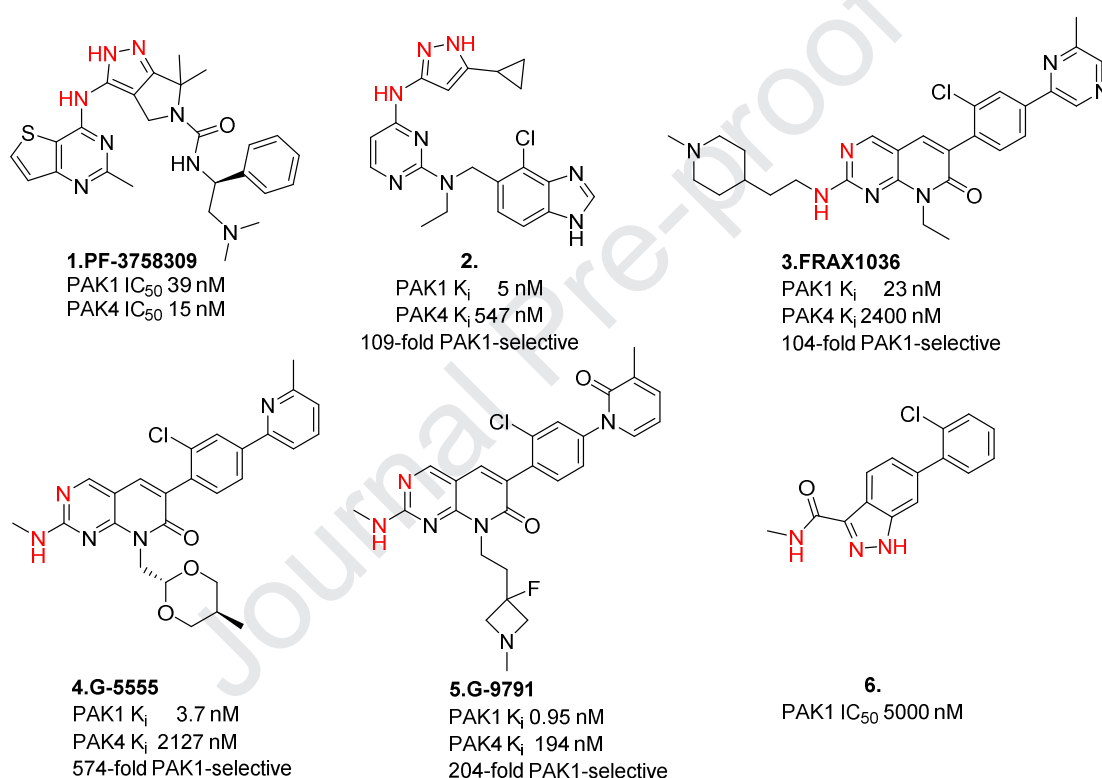
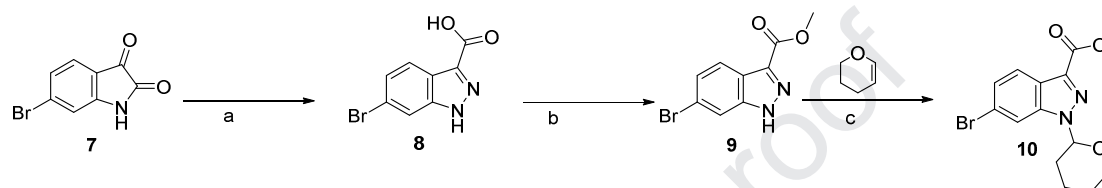


**Fig. 1.** Structures of representative PAK1 inhibitors and general structure of the compounds designed in this study.

In the present study, we reported a new structural chemotype containing the 6-(2-chlorophenyl)-1*H*-indazole-3-carboxamide scaffold for inhibitory activity and isoform selectivity of PAK1 by a fragment-based virtual screening strategy. The design, synthesis and structure-activity relationship studies that led to the discovery of representative compound **301** are described. Furthermore, we also explored the anti-tumour effects of the **301** on the proliferation and migration/invasion, as well as the possible mechanism of action. It is expected that **301** derivatives can be promising scaffolds for development of PAK1 selective inhibitors.

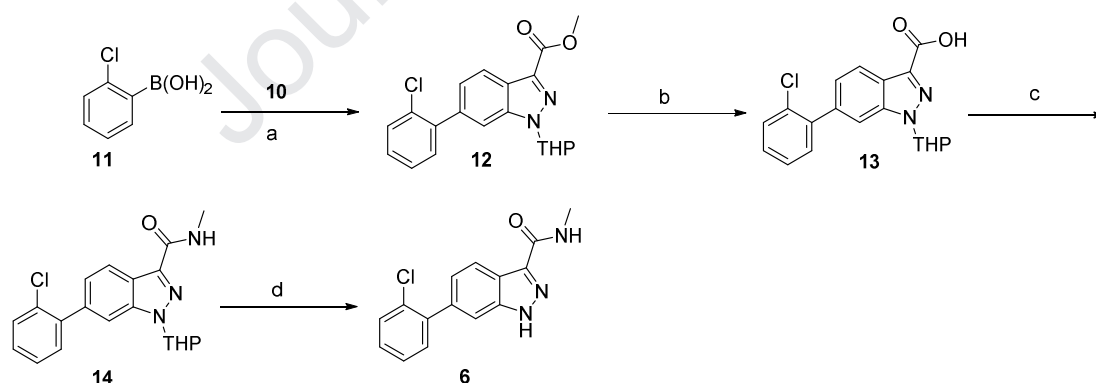
## 2. Chemistry

The synthesis route of the THP-protected 1*H*-indazole-3-carboxylate scaffold is described in **Scheme 1**. Compound **8** was obtained by treating the available compound **7** using a three-step procedure: cleavage with aqueous sodium hydroxide, diazotization with aqueous sodium nitrite in hydrochloric acid, and finally the reduction and cyclization of the intermediate diazonium salts with a cooled solution of tin(II) chloride dihydrate in hydrochloric acid. Then, the product was esterified to obtain compound **9** under reflux conditions in methanol, which was converted to the THP-protected intermediate **10** [22, 23].



**Scheme 1.** Reagents and conditions: (a) (i) NaOH, H<sub>2</sub>O, 50 °C, 1 h; (ii) HCl, NaNO<sub>2</sub>, H<sub>2</sub>O, 0 °C, 1 h; (iii) SnCl<sub>2</sub>, HCl, 25 °C, 2 h. (b) SOCl<sub>2</sub>, MeOH, 65 °C, 5 h. (c) TsOH, CH<sub>3</sub>CN, 25 °C, 2 h.

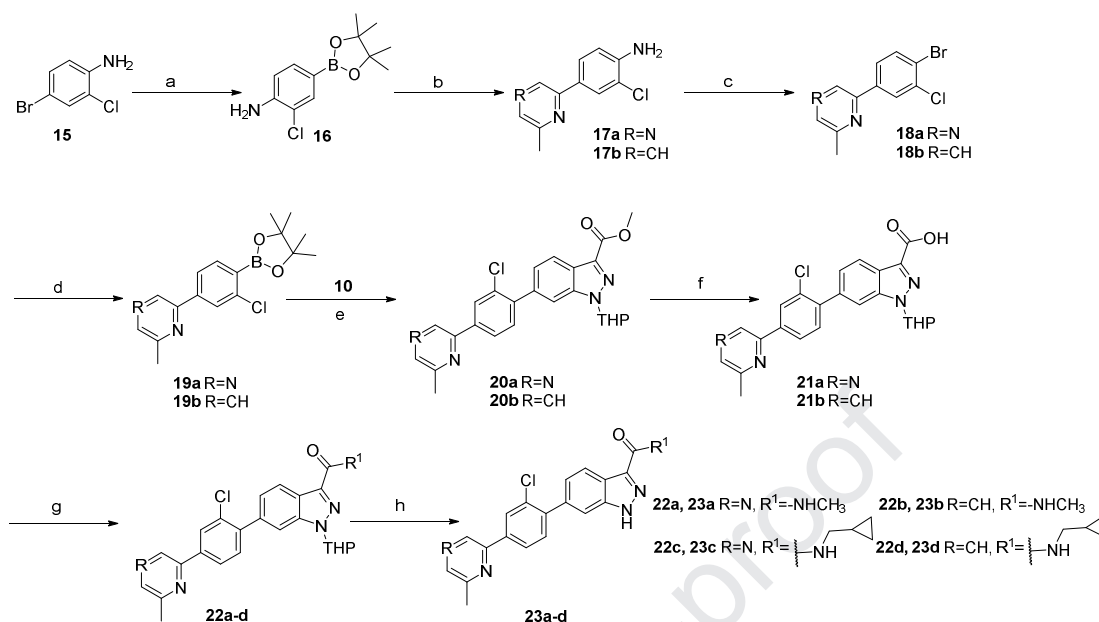
The synthesis route for compound **6** is shown in **Scheme 2**. Compound **12** was obtained from the starting material through the Suzuki coupling reaction [24]. Then, it was converted to the amide **14** through hydrolysis and amide coupling reactions. Deprotection using HCl cleavage of the hemiaminal intermediate afforded the final compound **6** [25].



**Scheme 2.** Reagents and conditions: (a) (2-chlorophenyl)boronic acid, Pd(dppf)Cl<sub>2</sub>, K<sub>2</sub>CO<sub>3</sub>, dioxane, H<sub>2</sub>O, 80 °C, 2 h; (b) NaOH, MeOH, H<sub>2</sub>O, 65 °C, 2 h; (c) CH<sub>3</sub>NH<sub>2</sub>, HATU, DIEA, DMF, 25 °C, 12 h; (d) HCl, MeOH, 65 °C, 12 h.

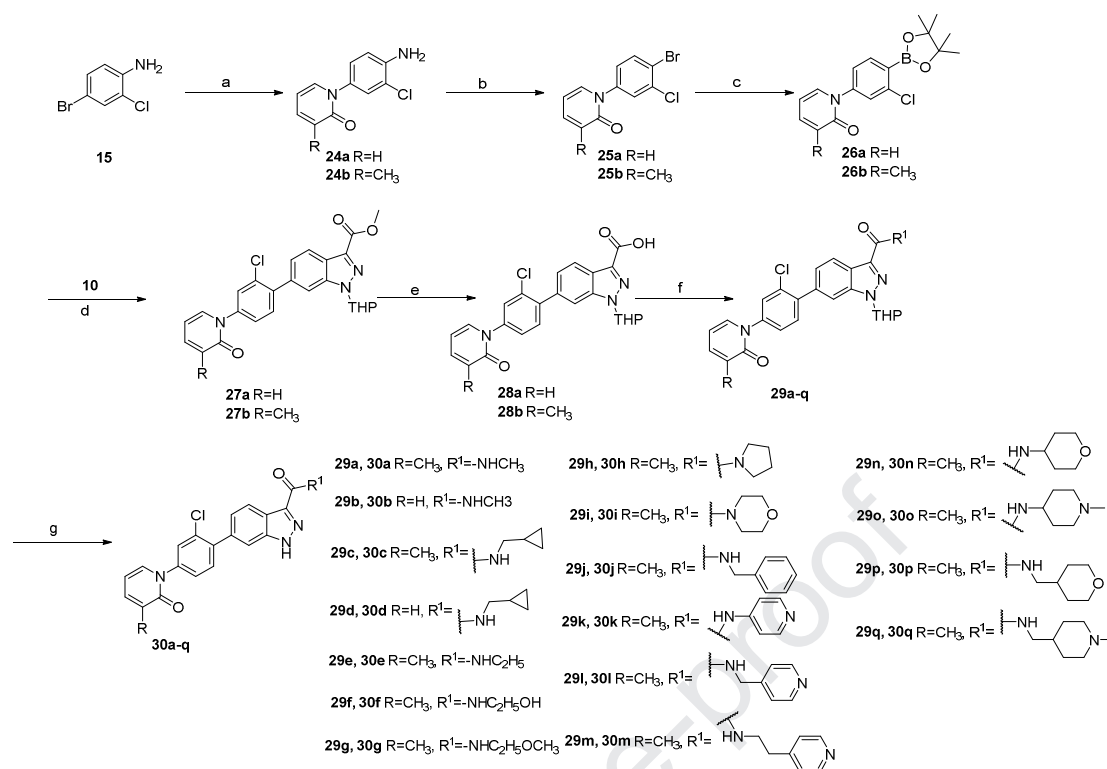
The synthesis routes of compounds **23a-d** are described in **Scheme 3**. Compound **15** was used to produce compound **17** in a 2-step Suzuki coupling reaction, which was then diazotized and brominated to yield compound **18** [26]. Then, compound **19** was prepared from compound **18** through the Suzuki coupling reaction. The final

compounds **23a-d** were prepared using a method similar to the procedure described for compound **6**.



**Scheme 3.** Reagents and conditions: (a) bis(pinacolato)diboron, AcOK, Pd(dppf)Cl<sub>2</sub>, dioxane, 110 °C, 12 h; (b) Pd(PPh<sub>3</sub>)<sub>4</sub>, K<sub>2</sub>CO<sub>3</sub>, dioxane, H<sub>2</sub>O, 80 °C, 2 h; (c) (i) HBr, NaNO<sub>2</sub>, 0 °C, 1 h and (ii) CuBr, HBr, 70 °C 2 h; (d) bis(pinacolato)diboron, AcOK, Pd(dppf)Cl<sub>2</sub>, dioxane, 110 °C, 12 h; (e) Pd(PPh<sub>3</sub>)<sub>4</sub>, K<sub>2</sub>CO<sub>3</sub>, dioxane, H<sub>2</sub>O, 80 °C, 2 h; (f) NaOH, MeOH, H<sub>2</sub>O, 65 °C, 2 h; (g) R<sup>1</sup>NH<sub>2</sub>, HATU, DIEA, DMF, 25 °C, 12 h; (h) HCl, MeOH, 65 °C, 12 h.

The synthesis routes of compounds **30a-q** are shown in **Scheme 4**. Compound **24** was synthesized from compound **15** using the Ullmann coupling reaction [27]. Then, it was diazotized and brominated to obtain compound **25**, which was installed using Suzuki coupling to obtain compound **26** [28, 29]. The final compounds **30a-r** were prepared using a method similar to the procedure used for compound **6**.



**Scheme 4.** Reagents and conditions: (a) CuI, *N,N*-dimethyl-1,2-ethanediamine, K<sub>3</sub>PO<sub>4</sub>, dioxane, 120 °C, 24 h; (b) (i) HBr, NaNO<sub>2</sub>, 0 °C, 1 h (ii) CuBr, HBr, 70 °C, 2 h; (c) AcOK, Pd(dppf)Cl<sub>2</sub>, bis(pinacolato)diboron, dioxane, 110 °C, 12 h; (d) Pd(dppf)Cl<sub>2</sub>, K<sub>2</sub>CO<sub>3</sub>, dioxane, H<sub>2</sub>O, 80 °C, 2 h; (e) NaOH, MeOH, H<sub>2</sub>O, 65 °C, 2 h; (f) R<sup>1</sup>NH<sub>2</sub>, HATU, DIEA, DMF, 25 °C, 12 h; (g) HCl, MeOH, 65 °C, 12 h.

### 3. Results and Discussion

#### 3.1. Hit identification and binding mode analysis

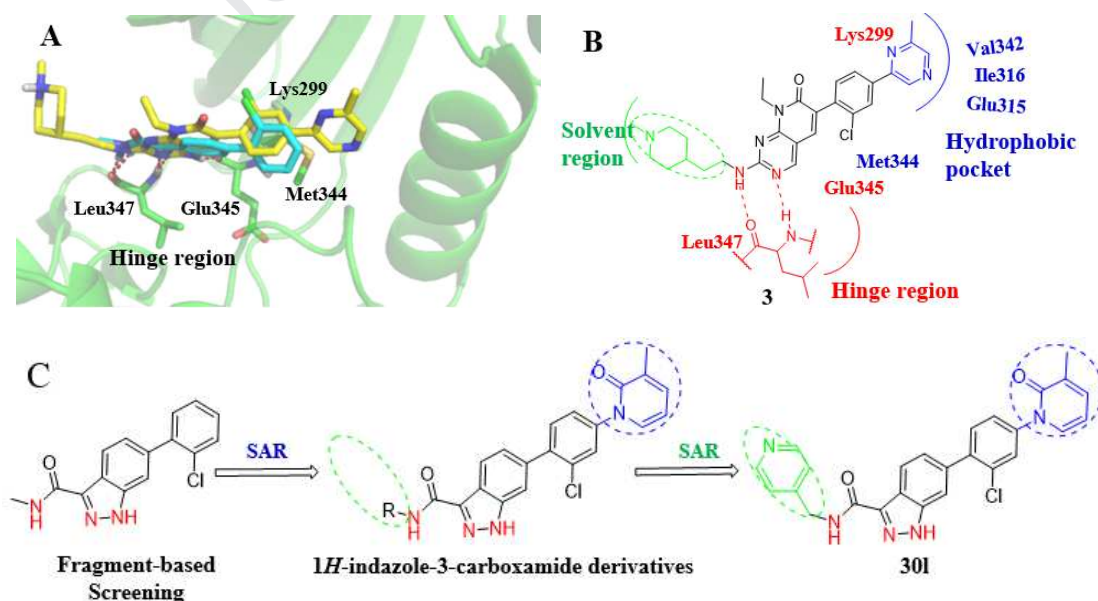
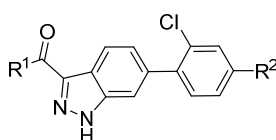


**Fig. 2.** (A) Predicted binding modes of FRAX1036 (**3**) and compound **6** in the ATP-binding site of PAK1. Overlay of compound **6** (cyan) and FRAX1036 (**3**) (yellow) bound in the PAK1 kinase active site (PDB code 5DEY). The ligands and important residues are shown in stick form. The hydrogen bonds are shown as red dashed lines. (B) A schematic illustrating the interaction between compound **3** and the surrounding residues within the binding pocket of PAK1. (C) Strategy used to design the series of 1*H*-indazole-3-carboxamide derivatives of PAK1 inhibitors.

An in-house hit fragment library consisting of 235 diverse fragment molecules was subjected to a virtual screening schedule for generating the starting molecule targeting PAK1 (**Fig. S1**). After a cluster analysis and visual inspection, 21 representative compounds (for details see Supplementary Material **Table S2**) with reasonable poses, Glide-Score value, physicochemical properties (i.e. molecular weight, topological polar surface areas, numbers of hydrogen bond acceptor and donor groups) and structure accessible were selected for further biological evaluation. In addition, these compounds passed the pan-assay interference compound (PAINS) substructure filtration. Among them, Hit 5, Hit 10 and Hit 12 showed potent inhibition activity against PAK1 with the inhibition ratio of higher than 80% at 10  $\mu\text{M}$  and were regarded as active scaffolds for PAK1. However, the structural modification space of Hit 5 is limited as pyrrole group is not convenient for introducing complementary chemical groups. B. Yang has reported the structural analogs of Hit 10 as PAK1 inhibitor [30]. Therefore, the 6-(2-chlorophenyl)-1*H*-indazole-3-carboxamide indazole scaffold (**6**) was a suitable hit compound due to its novel structure and large chemical space for modification. From the docking prediction, compound **6** formed conserved hydrogen bonds with the PAK1 kinase hinge residues Glu345 and Leu347 (**Fig. 2A**), while the aromatic ring of the chlorophenyl moiety was refined in the hydrophobic side chains consisting of the Met344 gatekeeper residue and Lys299 catalytic residue. These results prompted us to choose compound **6** as a starting point for optimization.

### 3.2. Scaffold modification and analysis of the structure-activity relationship

**Table 1.** Optimization of the substitutions on the hydrophobic moiety.



Compound	R <sup>1</sup>	R <sup>2</sup>	PAK1 IC <sub>50</sub> ( $\mu\text{M}$ ) <sup>a</sup>	clogP <sup>b</sup>	tPSA( $\text{\AA}$ ) <sup>c</sup>
<b>6</b>	-NHCH <sub>3</sub>	H	5	3.6	53.5

<b>23a</b>	-NHCH <sub>3</sub>		0.159	3.7	78.2
<b>23b</b>	-NHCH <sub>3</sub>		0.052	4.7	65.9
<b>23c</b>			0.777	4.7	78.2
<b>23d</b>			0.229	5.7	65.9
<b>30a</b>	-NHCH <sub>3</sub>		0.016	3.9	73.8
<b>30b</b>	-NHCH <sub>3</sub>		0.330	3.4	73.8
<b>30c</b>			0.034	4.9	73.8
<b>30d</b>			0.590	4.4	73.8
<b>FRAX1036</b>	-	-	0.023 <sup>e</sup>	3.6	53.5
<b>Staurosporine<sup>d</sup></b>	-	-	(0.0006) <sup>f</sup>	3.7	69.8
<b>PF-3758309<sup>d</sup></b>	-	-	0.052/ (0.036) <sup>f</sup>	4.3	98.3

<sup>a</sup> IC<sub>50</sub> values were determined using Kinase HotSpot Profiling assays. <sup>b</sup> The clogP values were calculated using the Qikprop software with the default settings (pH = 7.0). <sup>c</sup> Topological polar surface area. <sup>d</sup> used as a positive control [31]. <sup>e</sup> K<sub>i</sub> values (nM). <sup>f</sup> reported data [31].

To design more potent derivatives, the binding modes of compound **6** and FRAX1036 in PAK1 were overlaid. We discerned that the hydrophobic moiety at the 6-position on the pyrido[2,3-d] pyrimidin-7-one of FRAX1036 was important for its binding to PAK1. Hence, we introduced similar moieties in the pyrazine moiety of FRAX1036 into compound **6** and the modified hydrophobic group was subjected to SAR analyses (**Table1**) to improve the inhibitory potency against PAK1 kinase (**Fig. 2C**).

We first incorporated hydrophobic moieties onto the chlorophenyl group of compound **6** to enlarge the fragment on the right side. The introduction of a 5-methyl-2-pyrazinyl group (**23a**) significantly increased the enzymatic potency ( $IC_{50} = 159$  nM) compared with compound **6** (**Table 1**), consistent with our hypothesis about the importance of a hydrophobic group at the 4-position of the 2-chloro-phenyl ring (**Fig. 2A** and **2B**). Subsequently, substitutions at the position including 5-methyl-2-pyridinyl (**23b**) and 5-methyl-2-pyridone (**30a**) groups slightly increased the enzymatic activities ( $IC_{50} = 52$  and  $16$  nM, respectively), implying that terminal hydrophobic ring might contribute to the PAK1 activity. Among these compounds, **30a** showed the most effective inhibition, with an  $IC_{50}$  value of  $16$  nM. The methyl substituent showed improved activity by filling a small hydrophobic pocket beside the ATP binding area during the optimization of the FRAX1036 structure [20]. We then removed the methyl group at the 3-position of pyridone to confirm the importance of the potential pocket. As expected, the elimination of the methyl group resulted in a slight decrease in the inhibitory potency against PAK1 ( $IC_{50} = 330$  nM) compared to compound **30a**. While investigating substitutions of the  $R^1$  position with a cyclopropylmethylene amine group, the compounds displayed similar or slightly decreased potency compared to that with the methyl amine group. Therefore, the 3-methylpyridone group was deemed best suited to reach a desirable enzyme potency during the optimization of hydrophobic groups in the indazole derivatives. We retained the 3-methylpyridone for further structural modification.

We docked compound **30a** into the ATP binding site of PAK1 to obtain insights into the putative binding mode of this inhibitor with the PAK1 kinase. As shown in **Fig. 3A**, obvious hydrogen bonds between the kinase hinge residues Glu345 and Leu347 of PAK1 were observed and identified as important interactions contributing to the inhibition of PAK1 activity. The chlorophenyl moiety fits suitably in the cleft formed by the hydrophobic chains of the Met344 gatekeeper residue, and the 3-methylpyridone moiety protrudes into the deep back pocket of the ATP binding site surrounded by Glu315, Ile316, and Val342. Additionally, the 3-methylpyridone group also forms a hydrogen bond with the catalytic Ly299 residue, thus improving the inhibitory potency against PAK1. Since the amide group is directed toward the bulk solvent pocket, the activity may be modulated through the optimization of this position for further drug development. Therefore, a group extending from the 1*H*-indazole-3-carboxamide indazole scaffold would be exposed to the solvent area and balance the inhibitory activity and drug-like properties.

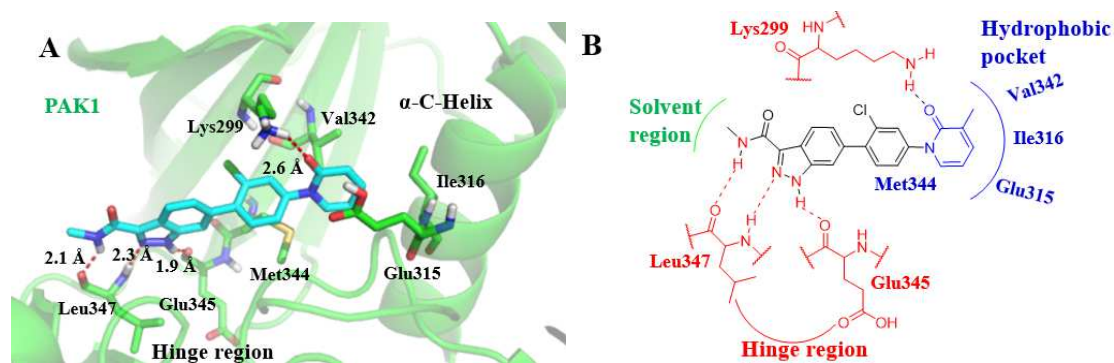


**Fig. 3.** (A) Predicted binding mode of compound **30a** in the ATP-pocket of PAK1 (PDB code 5DEY). The ligands and important residues are shown in stick form. The hydrogen bonds are shown as red dashed lines. (B) A schematic illustrating the interactions between compound **30a** and the surrounding residues within the binding site of PAK1.

Based on compound **30a**, we next turned our attention to further study the SAR of amide groups (**Table 2**). Various amines were utilized to replace the methyl amine in compound **30a**. Compounds **30e-30g** with ethyl amide, 2-hydroxyethyl amide or 2-methoxyethyl amide groups were 3-5-fold less potent inhibitors of PAK1 than compound **30a**. However, the PAK1 inhibitory potency nearly completely disappeared in compounds containing the cyclic secondary amines (**30h-30i**). We speculated that the amide NH group would function as a crucial hydrogen bond donor and interact with Leu347 in the hinge region of PAK1. As shown in **Fig. S2**, compounds **30h-30i** lacked a key hydrogen bond in the hinge region, resulting a direct loss of activity of these compounds. Interestingly, compounds **30n** and **30o** regained their enzyme inhibitory activity ( $IC_{50} = 744$  nM and 143 nM, respectively) upon the reintroduction of a primary amine group. Based on these results, the amide NH group was beneficial for increasing the potency, and the solvent area of the compound also participated in PAK1 activity. Subsequently, the length of the linker was explored by comparing compounds **30p** and **30q**. The inclusion of the methylpiperidine group appeared to increase the PAK1 inhibitory activity ( $IC_{50} = 22$  nM), suggesting that the flexibility of the attached group might improve PAK1 inhibition upon the introduction of the cyclic hydrophilic moiety. The saturated alkyl ring was replaced with pyridyl amine groups in compounds **30k-30m** to further explore the effect of the aromatic substituent. These compounds exhibited similar or improved inhibitory potencies ( $IC_{50} = 16$  nM, 9.8 nM and 21 nM, respectively) compared to **30a**. However, the replacement of the pyridine group with a phenyl hydrophilic group led to 10-fold decrease in potency (**30j**). The potency of this analogue was lost due to the requirement for a highly polar group in

the PAK1 solvent pocket. Finally, compounds **30a**, **30c**, **30e** and **30l** displayed excellent enzyme potency and would be candidates for a detailed evaluation.

**Table 2.** Studies of the structure-activity relationship after replacing the methyl amine group with various amine derivatives in the hydrophilic moiety

Compound	R	PAK1 IC <sub>50</sub> (μM) <sup>a</sup>	clogP <sup>b</sup>	tPSA (Å) <sup>c</sup>
<b>30e</b>	-NHC <sub>2</sub> H <sub>5</sub>	0.045	4.5	73.8
<b>30f</b>	-NHC <sub>2</sub> H <sub>5</sub> OH	0.066	3.4	94.0
<b>30g</b>	-NHC <sub>2</sub> H <sub>5</sub> OCH <sub>3</sub>	0.071	4.1	83.0
<b>30h</b>		>10	4.1	65.0
<b>30i</b>		>10	3.6	74.2
<b>30n</b>		0.744	3.6	83.0
<b>30o</b>		0.143	4.0	77.0
<b>30p</b>		0.042	4.2	83.0
<b>30q</b>		0.022	4.6	77.0
<b>30k</b>		0.016	4.7	86.2
<b>30l</b>		0.0098	4.4	86.2
<b>30m</b>		0.021	4.5	86.2
<b>30j</b>		0.092	5.9	73.8
<b>FRAX1036</b>	-	0.023 <sup>e</sup>	3.6	53.5
<b>Staurosporine<sup>d</sup></b>	-	(0.0006) <sup>f</sup>	3.7	69.8
<b>PF-3758309<sup>d</sup></b>	-	0.052	4.3	98.3

<sup>a</sup> IC<sub>50</sub> values were determined using Kinase HotSpot Profiling assays. <sup>b</sup> The clogP values were calculated using Qikprop software with the default settings (pH = 7.0). <sup>c</sup> Topological polar surface area. <sup>d</sup> used as a positive control. <sup>e</sup> K<sub>i</sub> values (nM). <sup>f</sup> reported data [31].

### 3.3. PAK subtype selectivity and hERG inhibition



**Fig. 4.** Sequence alignment of the kinase domains of PAK1 and PAK4. Identical residues between the two kinases are highlighted in green boxes. Different residues are shown with a white background. The red stars label key residues of the hinge regions in PAK1 and PAK4. The helices are shown in red and  $\beta$  strands are shown in cyan.

Sequences analysis of the PAK1 and PAK4 kinase domains revealed that PAK1 shared 72% sequence similarity with PAK4 in the kinase domain (**Fig. 4**). As was mentioned before, PAK1 subtype-selective inhibitors possess pharmacological advantages over pan-PAK inhibitors. We then examined the kinase subtype selectivity for potent compounds. As shown in **Table 3**, these compounds were highly active PAK1 inhibitors, but did not inhibit PAK4 (IC<sub>50</sub> > 10  $\mu$ M). The four compounds exhibited comparable subtype selectivity to FRAX1036, while compound **30l** displayed a more favourable PAK1 specificity (1000-fold greater over PAK4).

**Table 3.** Selectivity and hERG profiles of selected compounds.

Compound	PAK1 IC <sub>50</sub> ( $\mu$ M) <sup>a</sup>	PAK4 IC <sub>50</sub> ( $\mu$ M) <sup>a</sup>	PAK1 Select.index <sup>b</sup>	hERG	clogP <sup>c</sup>	tPSA ( $\text{\AA}$ ) <sup>d</sup>
				% inh. @ 10 $\mu$ M /IC <sub>50</sub> ( $\mu$ M)		
<b>30a</b>	0.016	>10	>625x	21.0	3.9	73.8
<b>30c</b>	0.034	>10	>290x	82.3	4.9	73.8
<b>30e</b>	0.045	>10	>200x	90.4	4.5	73.8
<b>30p</b>	0.042	ND <sup>e</sup>	ND	42.1	4.2	83.0

<b>301</b>	0.010	>10	>1000x	16.0	4.4	86.2
<b>FRAX1036</b>	0.023 <sup>f</sup>	2.4 <sup>f</sup>	105x <sup>g</sup>	89% <sup>h</sup>	3.6	53.5
<b>Staurosporine</b> <sup>i</sup>	(0.0006) <sup>h</sup>	(0.06) <sup>h</sup>	10x	ND	3.7	69.8
<b>PF-3758309</b> <sup>i</sup>	0.052/ (0.036) <sup>h</sup>	0.038/ (0.015) <sup>h</sup>	0.73x 0.42x	41.1	4.3	98.3

<sup>a</sup> IC<sub>50</sub> values were determined using Kinase HotSpot Profiling assays. <sup>b</sup> PAK4 IC<sub>50</sub>/ PAK1 IC<sub>50</sub>, x = fold. <sup>c</sup> The clogP values were calculated using Qikprop software with the default settings (pH = 7.0). <sup>d</sup> Topological polar surface area. <sup>e</sup> ND = not determined. <sup>f</sup> K<sub>i</sub> values (nM) [31]. <sup>g</sup> PAK4 K<sub>i</sub>/ PAK1 K<sub>i</sub>, x = fold. <sup>h</sup> reported data [31]. <sup>i</sup> used as a positive control.

### 3.4. Kinase selectivity assessment

We further screened the selectivity of **301** against a panel of 29 kinases including PAK1 signal pathways-related, the high structural homology of PAK1 and wide-used marketed drug-related kinase using the Kinase HotSpot Profiling assays (Table 4). It was found that compound **301** did not show obvious inhibition on these tested kinases except that it displayed moderate inhibition on PAK2, PAK3 at 0.1 μM, which were also the group I PAK family. The data indicated that **301** had good selectivity profile. Taken together, the data demonstrated that **301** was a potent and selective PAK1 inhibitor.

**Table 4.** Kinase selectivity profile of compound **301**.

Kinase	% Enzyme Activity <sup>a</sup> (0.1 μM)	Kinase	% Enzyme Activity <sup>a</sup> (0.1 μM)
ABL1	106.39	JNK1	72.75
AKT1	98.85	KDR/VEGFR2	92.41
ALK	96.99	LCK	88.64
Aurora A	87.80	LIMK1	115.26
AXL	88.41	MEK1	84.39
BRAF	84.41	MST3/STK24	63.96
BTK	99.13	P38a/MAPK14	77.96
c-Kit	99.18	PAK1	27.55

CDK6/cyclin D1	111.75	PAK2	27.98
EGFR	89.31	PAK3	33.90
EPHA1	91.90	PAK4	103.71
ERK1	98.96	PAK5	116.44
FLT3	98.77	PAK6	80.02
HPK1/MAP4K1	89.62	SYK	94.16
JAK1	88.65		

<sup>a</sup> Values are reported as the averages of two independent experiments.

### 3.5. *In vitro* assessment of the antiproliferative activities

Following the SAR analysis of newly synthesized compounds and *in vitro* kinase assay, those compounds with IC<sub>50</sub> values for PAK1 that were less 150 nM were tested for their antiproliferative activity against the MDA-MB-231 and HCT-116 cell lines (**Table 5**), which were PAK1 overexpressed tumour cells [5, 15]. Unfortunately, these compounds exhibited limited inhibitory activity, with an inhibition ratio less than 20% at 1  $\mu$ M. The poor antiproliferative activity of the potent PAK1 compound might be attributed to minor contribution of PAK1 to tumour proliferation [3, 32]. Further analyses of the anti-tumour efficiency for this series of PAK1 inhibitors were performed by examining the anti-tumour metastatic effect.

**Table 5.** Antiproliferative activity against MDA-MB-231 and HCT-116 cells *in vitro*.

Compound	MDA-MB-231	HCT-116	Compound	MDA-MB-231	HCT-116
	Inhibition % (1 $\mu$ M) <sup>a</sup>	Inhibition % (1 $\mu$ M) <sup>a</sup>		Inhibition % (1 $\mu$ M) <sup>a</sup>	Inhibition % (1 $\mu$ M) <sup>a</sup>
<b>30a</b>	13.18±0.57	17.23±0.64	<b>30q</b>	18.40±0.26	20.12±2.35
<b>30c</b>	6.87±0.81	10.75±0.47	<b>30k</b>	6.59±0.65	4.41±0.56
<b>30e</b>	10.20±0.87	9.37±0.51	<b>30l</b>	6.31±0.57	8.73±0.52
<b>30f</b>	17.36±0.69	19.23±1.27	<b>30m</b>	8.42±0.32	15.29±1.47
<b>30g</b>	3.07±0.26	10.29±2.36	<b>30j</b>	9.66±0.46	13.15±3.26
<b>30n</b>	19.19±0.77	7.91±1.52	<b>23a</b>	15.26±0.59	11.49±1.57
<b>30p</b>	9.45±0.23	16.18±0.45	<b>23b</b>	8.12±0.37	7.16±0.17

PF-3758309<sup>b</sup> 62.60±1.43 83.20±4.26

<sup>a</sup>Each compound was tested in duplicate and the data are presented as the means ± SD; <sup>b</sup>used as a positive control.

### 3.6. Effects of compound 301 on cell migration and invasion

The relatively low cell growth inhibitory activities suggested that PAK1 might not be the “driving force” for tumorigenesis and tumour growth, consistent with the oncogenic function mentioned above. Based on accumulating evidence, PAK1 is definitely required for tumour metastasis [5, 33-35], which remains a substantial challenge for the treatment of tumours. As compound **301** represents a new chemical type of PAK1 kinase inhibitor with a high level of PAK1 inhibitory activity, an evaluation of its anti-metastasis effect would be interesting. We then performed wound healing assays in MDA-MD-231 and HCT-116 cells treated with different concentrations of compounds. The distance migrated was measured using ImageJ software. As shown in **Fig. 5A and Fig. S3**, wound healing was suppressed by treatments with the compound at 1 μM in a dose-dependent manner.

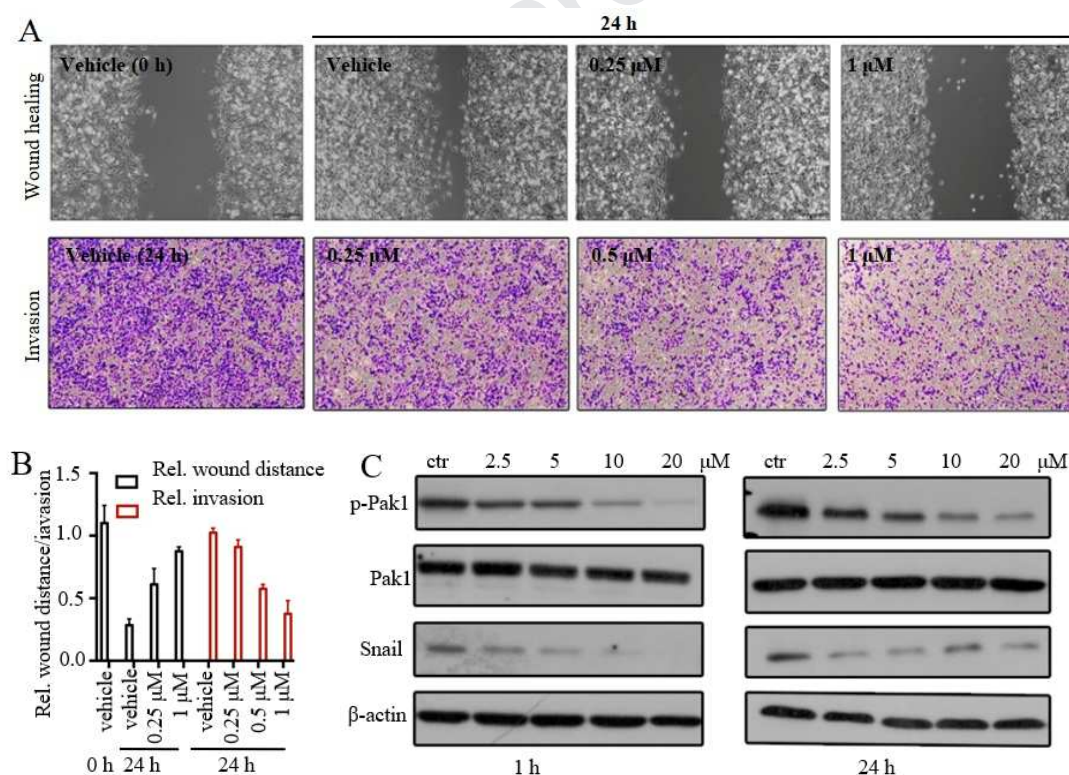


**Fig. 5.** (A) The migration and invasion capacities of **301** in MDA-MB-231 cells were tested using wound healing assays and Transwell assays, respectively, after 24 h of treatment with the indicated concentrations. (B) The distance migrated in the wound healing assay and the number of penetrated cells in the Transwell assay were counted, respectively. The results are presented as means ± standard deviations. (C) The levels of proteins involved in PAK1 related signalling

pathways in MDA-MB-231 cells after treatment with compound **301** for 1 h or 24 h.  $\beta$ -actin served as the loading control.

Transwell invasion assays were performed to analyse the capacity of cell motility and invasiveness toward a **301** attractant gradient. The numbers of tumour cells that penetrated through the matrigel and migrated to the other side of the filter membrane were quantified. A significant decrease in the number of penetrated cells (less than 40%) was observed after 24 h of treatment with different concentrations of compound **301** (**Fig. 5B**). Together with the low level of cytotoxicity in the cell proliferation assay at the same concentration, the anti-tumour effect of compound **301** was mainly due to the inhibition of cell migration. Collectively, compound **301** possessed potent anti-metastatic ability against PAK1-related tumour cells and provided a potential application for tumour treatment.

### 3.7. Analysis of the Mechanism of Action of compound **301**

After confirming the on-target activity of the 1*H*-indazole-3-carboxamide derivative **301** against the PAK1 protein and potential anti-tumour metastasis profile, we further investigated whether compound **301** inhibited PAK1 in cells. As expected, it decreased the levels of activated PAK1 (PAK<sup>P-Ser144</sup>) in a dose-dependent manner (**Fig. 5C**) when MDA-MB-231 cells were exposed to different concentrations of compound **301**, confirming the on-target behaviour of **301** in tumour cells. Recent studies have shown the modulation of the downstream EMT-related signal pathways upon PAK1 deactivation [5, 10]. The zinc finger protein Snail is one of the critical indicators of the EMT, allowing cells to detach from their neighbours and migrate [10]. PAK1 phosphorylation promotes Snail expression, thereby regulating the metastatic potential of tumor cells [10, 36]. We monitored the Snail expression in MDA-MB-231 cells treated with compound **301** to clarify the cellular activity of compound **301** in inhibiting the PAK1-induced EMT. As evident from **Fig. 5C**, the level of the Snail protein was reduced in cells treated with 2.5, 5, 10 and 20  $\mu$ M compound **301** for both 1 h and 24 h compared to untreated cells, indicating that the EMT process is indeed impaired, thereby decreasing the migration and invasion of MDA-MB-231 cells. Importantly, the potency of compound **301** in reducing tumour invasion was evaluated at a relatively low concentration that does not inhibit cell proliferation. Based on these results, compound **301** functions as promising PAK1 inhibitor by blocking tumour metastasis through Snail downregulation and could serve as a lead compound for drug discovery.

### 3.8. *In silico* binding mode of **301**

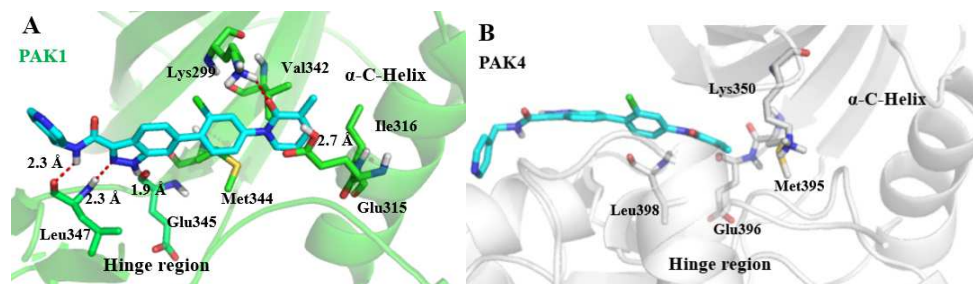


**Fig. 6.** (A) Predicted docking model of compound **301** in the ATP-binding pocket of PAK1 or (B) PAK4. Protein residues are shown as green sticks (PAK1) or grey sticks (PAK4) with labelled names. The hydrogen bonds are shown as red dashed lines.

Molecular docking of the representative compound **301** in the PAK1 and PAK4 kinase domains was performed to exploit the structural basis of the isoform selectivity. As shown in **Fig. 6A** and **6B**, compound **301** forms conserved hydrogen bond interactions with the kinase hinge residues Glu345 and Leu347 of PAK1, which is important for PAK1 inhibition, but it does not interact with Glu396 and Leu398 in the hinge region of PAK4. Despite the similar architecture of the ATP binding pockets between the two proteins, the back pocket of PAK1 is more extensive than in PAK4, which enables the 2-chloro-4-(3-methyl-2-oxopyridin-1(2*H*)-yl) phenyl moiety of compound **301** to occupy the pocket with its extended hydrophobic groups. Additionally, the carbonyl group in the 3-methylpyridone moiety of compound **301** forms an additional hydrogen bond interaction with the catalytic Lys299 residue of PAK1 that improves the inhibitory potency against PAK1.

To better understand the stability of **301** with PAK family, we performed molecular dynamics (MD) simulation for monitoring its binding with PAK1 and PAK4 at 50 ns (nanosecond) scale. RMSF and Molecular mechanics generalized born/surface area (MM\_GBSA) binding free energy were calculated to investigate the selective binding mechanism of **301** to the ATP-binding site of PAK1 over PAK4. As shown in **Fig. 7**, the PAK1 or PAK4 protein reached equilibrium stage after 10 ns of simulation trajectory. The RMSD values eventually became stable and were about 2.71 Å and 1.96 Å, respectively, for PAK1 and PAK4 (**Fig. 7A**). The conformation of **301** also exhibited stability with the values of 2.1 Å and  $0.99 \pm 0.19$  Å (**Fig. 7B**) in the ATP-binding site of PAK1 and PAK4 thus indicating that the MD simulation model was reliable. The RMSF values of PAK1 key residues (Leu347, Glu345, Met344, Val342, Lys299, Glu315 and Ile316) contributing to the binding interaction were significantly smaller than the corresponding PAK4 residues (**Fig. 7C**), implied the compound **301** possessed more potent on stabilizing PAK1 protein. By comparative analysis on the GB binding-free energies ( $\Delta G$  prep), we found that the predicted  $\Delta G$

of **301** in PAK1 were calculated to be -57.62 kcal/mol, which was also lower than that of PAK4 (-32.12 kcal/mol, **Table S2**). These results suggested compound **301** had high binding affinity to PAK1 than PAK4 and were consistent with the actual bioactivities.

Collectively, these differences in the binding to PAK1 and PAK4 provide an explanation for the high potency and selectivity of compound **301** toward PAK1.

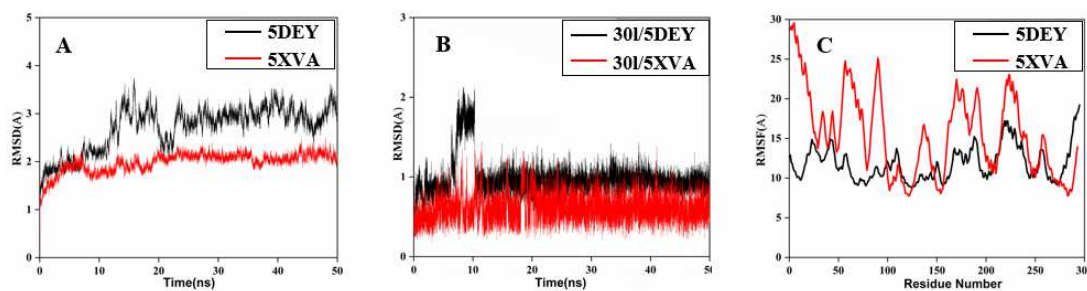


**Figure 7.** The time dependence of RMSDs for PAK1 (black) and PAK4 (red) (A); and **301** in the ATP-binding site of PAK1 (black) and PAK4 (red) (B) during the 50 ns MD simulations; The RMSF (C) of each residue of the protein for the complex obtained from PAK1/**301** (black) and the PAK4/**301** (red). One nm is equal to 10 Å.

#### 4. Conclusions

In summary, we designed, synthesized and evaluated the biological effects of a series of 1*H*-indazole-3-carboxamide derivatives as an unexplored chemotype for PAK1 inhibitors. The molecular modelling suggested that PAK1 contains a large hydrophobic region in the deep back pocket surrounded by Glu315, Ile316, Val342, Met344 and Lys299, which maybe is crucial for its selectivity. Further SAR studies revealed that the incorporation of a large hydrophobic group particularly improved the inhibitory activity and selectivity toward PAK1. We successfully identified **301** as PAK1 selective inhibitor with powerful PAK1 inhibition ( $IC_{50} = 9.8$  nM) and high selectivity. The binding modes were also proposed through molecular docking and MD simulations and rationalized the preceding SAR. Notably, **301** displayed low hERG channel activity, which implied the safety of the compound. Its specificity and safety were further illustrated by low inhibitory effect on the tumour cell viability. However, this selected compound **301** effectively suppressed the migration and invasion of human MDA-MB-231 and HCT116 cancer cells due to its ability to decrease the level of phosphorylated PAK1 and then attenuated the expression of Snail. Our findings provided molecular insights into PAK1 drug design with the new structure type of the 1*H*-indazole-3-carboxamide moiety. **301** with its favourable biological performance might serve as a qualified anti-tumour metastasis lead compound for further investigation.

## 5. Experimental

### 5.1. Chemistry

All reagents and solvents were purchased from commercial suppliers and used without further purification. The reactions were monitored by TLC (Merck Kieselgel GF254) and spots were visualized with UV light; Isolation and purification of the compounds were performed by flash column chromatography on silica gel 60 (200-400 mesh). Melting points were determined by X-4 digital display micro-melting point apparatus (Beijing Tech Instrument Co., Ltd.); The structures of synthesized compounds were characterized by  $^1\text{H}$  NMR,  $^{13}\text{C}$  NMR, MS and HRMS. NMR spectra were recorded on Bruker AVANCE AV-400 spectrometer (400 MHz for  $^1\text{H}$ , 101 MHz for  $^{13}\text{C}$ ) or Bruker AVANCE AV-300 spectrometer (300 MHz for  $^1\text{H}$ , 75 MHz for  $^{13}\text{C}$ ); Mass spectra were obtained on the Agilent 1100 LC / MSD mass spectrometer (Agilent, USA) or Q-tofmicro MS (micromass company).

**6-Bromo-1H-indazole-3-carboxylic acid (8)** To a stirring solution of NaOH (0.386 g, 19.3 mmol) in  $\text{H}_2\text{O}$  (10 mL) was added 6-bromoindoline-2,3-dione **7** (2.00 g, 17.7 mmol). The resulting mixture was heated to 50 °C and stirred for 1 h. HCl (3.2 mL) was added under ice-cooling, then  $\text{NaNO}_2$  (0.610 g, 17.7 mmol) in  $\text{H}_2\text{O}$  (2 mL) was added dropwise for 0.5 h. Reaction was stirred under ice-cooling for 1 h.  $\text{SnCl}_2 \cdot 2\text{H}_2\text{O}$  (4.98 g, 44.24 mmol) in HCl (6 mL) was added dropwise for 10min. The mixture was stirred for 2 h at 25 °C. Upon completion, the mixture was filtered and rinsed with  $\text{H}_2\text{O}$ , then the precipitate was collected as crude product which was used for next step directly. Yield: 91%.

**Methyl 6-bromo-1H-indazole-3-carboxylate (9)** To the solution of compound **8** (2.00 g) in methanol (20 mL) were added  $\text{SOCl}_2$  (5 mL). Reaction mixture was heated to reflux and stirred for 6 h. Upon completion, the residue was taken up in ice water (60 mL). The pH was adjusted to 9-10 with saturated sodium carbonate solution. The aqueous phase was extracted with ethyl acetate (80 mL  $\times$  3). The combined organic extracts were washed with brine (40 mL  $\times$  3), dried over anhydrous  $\text{Na}_2\text{SO}_4$  and concentrated in vacuo. The residue was purified by silica gel column chromatography (n-hexane/ethyl acetate, 5/1) to afford title compound as a yellow solid. Yield: 79%.  $R_f$ : 0.46 (n-hexane/ethyl acetate, 4/1, v/v).  $^1\text{H}$  NMR (300 MHz,  $\text{DMSO}-d_6$ )  $\delta$ : 14.10 (br, 1H), 8.01 (d,  $J = 8.5$  Hz, 1H), 7.93 (d,  $J = 1.8$  Hz, 1H), 7.46 (dd,  $J = 8.5, 1.8$  Hz, 1H), 3.93 (s, 3H). MS (m/z):  $[\text{M}+\text{H}]^+$  255.1.

**Methyl 6-bromo-1-(tetrahydro-2H-pyran-2-yl)-1H-indazole-3-carboxylate (10)** To the solution of compound **9** (2.00 g, 7.84 mmol) in anhydrous ACN (50 mL) were added DHP (1.32 g, 15.69 mmol) and TsOH (0.135 g, 0.784 mmol). Reaction mixture was stirred at 25 °C for 2 h. Upon completion, the solvent was removed in vacuo, and the residue was extracted with ethyl acetate (60 mL  $\times$  3). The combined organic extracts were washed with brine (30 mL  $\times$  3), dried

over anhydrous  $\text{Na}_2\text{SO}_4$  and concentrated in vacuo. The residue was purified by silica gel column chromatography (n-hexane/ethyl acetate, 10/1) to afford title compound as a yellow solid. Yield: 85%.  $R_f$ : 0.32 (n-hexane/ethyl acetate, 10/1, v/v).  $^1\text{H}$  NMR (300 MHz,  $\text{DMSO}-d_6$ )  $\delta$ : 8.22 (s, 1H), 8.01 (d,  $J = 8.7$ , 1H), 7.52 (d,  $J = 8.6$  Hz, 1H), 6.03 (d,  $J = 9.4$ , 1H), 3.94 (s, 3H), 3.84 (m, 2H), 2.34 (m, 1H), 2.00 (m, 2H), 1.73 (m, 1H), 1.61 (m, 2H). MS (m/z):  $[\text{M}+\text{H}]^+$  339.1.

**Methyl 6-(2-chlorophenyl)-1-(tetrahydro-2H-pyran-2-yl)-1H-indazole-3-carboxylate (12)** To the solution of compound **10** (0.500 g, 1.47 mmol) in dioxane (20 mL) and  $\text{H}_2\text{O}$  (20 mL) were added compound **11** (0.276 g, 1.77 mmol),  $\text{K}_2\text{CO}_3$  (0.611 g, 4.42 mmol) and  $\text{Pd}(\text{dppf})\text{Cl}_2$  (0.0538 g, 0.0735 mmol). The resulting mixture was heated to 80 °C under a nitrogen atmosphere for 4 h. Upon completion, the solvent was removed in vacuo, and the residue was extracted with ethyl acetate (60 mL  $\times$  3). The combined organic extracts were washed with brine (30 mL  $\times$  3), dried over anhydrous  $\text{Na}_2\text{SO}_4$  and concentrated in vacuo. The residue was purified by silica gel column chromatography (n-hexane/ethyl acetate, 10/1, v/v) to afford title compound as a yellow solid. Yellow solid was afforded as the crude product which was used in next step.

**6-(2-Chlorophenyl)-1-(tetrahydro-2H-pyran-2-yl)-1H-indazole-3-carboxylic acid (13)** To the solution of compound **12** (0.300 g, 0.811 mmol) in MeOH (10 mL) and  $\text{H}_2\text{O}$  (10 mL) were added NaOH (0.162 g, 4.05 mmol). Reaction mixture was stirred at 65 °C for 12 h. Upon completion, the solvent was removed in vacuo. The pH was adjusted to 4-5 with AcOH solution. The aqueous phase was extracted with ethyl acetate (80 mL  $\times$  3). The combined organic extracts were washed with brine (40 mL  $\times$  3), dried over anhydrous  $\text{Na}_2\text{SO}_4$  and concentrated in vacuo. Yellow solid was afforded as the crude product which was used in next step.

**6-(2-Chlorophenyl)-N-methyl-1-(tetrahydro-2H-pyran-2-yl)-1H-indazole-3-carboxamide (14)** To the solution of compound **13** (0.200 g, 0.562 mmol) in dry DMF (20 mL) were added HATU (0.427 g, 1.12 mmol), DIEA (0.217 g, 1.69 mmol) and 2 M  $\text{CH}_3\text{NH}_2$ -MeOH (0.5 mL, 32.2 mmol). Reaction mixture was stirred at 25 °C for 12 h. Upon completion, the reaction mixture was quenched with ethyl acetate (80 mL), which was washed with water (40 mL  $\times$  3) and brine (40 mL  $\times$  3) successively, dried over anhydrous  $\text{Na}_2\text{SO}_4$ , filtered and concentrated in vacuo. Yellow solid was afforded as the crude product which was used in next step.

**6-(2-Chlorophenyl)-N-methyl-1H-indazole-3-carboxamide (6)** To the solution of compound **14** (0.100 g, 0.271 mmol) in MeOH (10 mL) and 2 M HCl (6 mL). The resulting mixture was heated to 65 °C for 4 h. Upon completion, the solvent was removed in vacuo. The pH was adjusted to 9-10 with saturated sodium carbonate solution. The aqueous phase was extracted with ethyl acetate (30 mL  $\times$  3). The combined organic extracts were washed with brine (20 mL  $\times$  3), dried over anhydrous  $\text{Na}_2\text{SO}_4$  and concentrated in vacuo. The residue was purified by silica gel column chromatography (n-hexane/ethyl acetate, 1/1, v/v) to afford title compound as a yellow solid.

Yield: 79%. mp: 228-233 °C. R<sub>f</sub>: 0.23 (n-hexane/ethyl acetate, 1/1, v/v). <sup>1</sup>H NMR (300 MHz, DMSO-*d*<sub>6</sub>) δ: 13.69 (s, 1H), 8.40 (q, *J* = 5.0 Hz, 1H), 8.23 (d, *J* = 8.4 Hz, 1H), 7.60 (m, 2H), 7.54 – 7.40 (m, 3H), 7.29 (d, *J* = 8.4 Hz, 1H), 2.84 (d, *J* = 4.5 Hz, 3H). HRMS-EI *m/z* [M+H]<sup>+</sup> calcd for C<sub>15</sub>H<sub>13</sub>ClN<sub>3</sub>O: 286.0669, found: 286.0742.

**2-Chloro-4-(4,4,5,5-tetramethyl-1,3,2-dioxaborolan-2-yl)aniline (16)** To the solution of compound **15** (2.00 g, 9.76 mmol) in dry dioxane (50 mL) were added Bis(pinacolato)diboron (2.97 g, 11.71 mmol), Potassium Acetate (2.87 g, 29.28 mmol) and Pd(dppf)Cl<sub>2</sub> (0.358g, 0.488 mmol) under an argon atmosphere. Reaction mixture was stirred at 100 °C for 12 h. Upon completion, the solvent was removed in vacuo, and the residue was extracted with ethyl acetate (60 mL × 3). The combined organic extracts were washed with brine (30 mL × 3), dried over anhydrous Na<sub>2</sub>SO<sub>4</sub> and concentrated in vacuo. Black solid was afforded as the crude product which was used in next step.

**2-Chloro-4-(6-methylpyrazin-2-yl)aniline (17a)** To the solution of compound **16** (2.00 g, 7.91 mmol) in dioxane (50 mL) and H<sub>2</sub>O (40 mL) were added 2-chloro-6-methylpyrazine (1.20 g, 9.49 mmol), K<sub>2</sub>CO<sub>3</sub> (3.27 g, 23.7 mmol), Pd(PPh<sub>3</sub>)<sub>4</sub> (0.457 g, 0.396 mmol) under an argon atmosphere. Reaction mixture was stirred at 80 °C for 6 h. Upon completion, the solvent was removed in vacuo, and the residue was extracted with ethyl acetate (60 mL × 3). The combined organic extracts were washed with brine (30 mL × 3), dried over anhydrous Na<sub>2</sub>SO<sub>4</sub> and concentrated in vacuo. The residue was purified by silica gel column chromatography (n-hexane/ethyl acetate, 4/1, v/v) to afford title compound as a yellow solid. Yield: 90%. R<sub>f</sub>: 0.26 (n-hexane/ethyl acetate, 2/1, v/v). <sup>1</sup>H NMR (300 MHz, DMSO-*d*<sub>6</sub>) δ: 8.91 (s, 1H), 8.34 (s, 1H), 8.01 (d, *J* = 2.0 Hz, 1H), 7.84 (dd, *J* = 8.5, 2.1 Hz, 1H), 6.89 (d, *J* = 8.5 Hz, 1H), 5.83 (s, 2H), 2.51 (s, 3H). MS (*m/z*): [M+H]<sup>+</sup> 220.2.

**2-Chloro-4-(6-methylpyridin-2-yl)aniline (17b)** The preparation of compound **17b** was similar with that of compound **17a** to afford title compound as a yellow solid. Yield: 86%. R<sub>f</sub>: 0.23 (n-hexane/ethyl acetate, 1/1, v/v). <sup>1</sup>H NMR (300 MHz, DMSO-*d*<sub>6</sub>) δ: 7.97 (m, 1H), 7.78 (m, 1H), 7.63 (m, 2H), 7.07 (d, *J* = 7.4 Hz, 1H), 6.86 (dd, *J* = 8.4, 1.8 Hz, 1H), 5.67 (s, 2H), 2.49 (s, 3H). MS (*m/z*): [M+H]<sup>+</sup> 219.3.

**2-(4-Bromo-3-chlorophenyl)-6-methylpyrazine (18a)** To a stirring solution of 48% of HBr (5 mL) and H<sub>2</sub>O (5 mL) were added compound **17a** (2.80 g, 12.84 mmol). The resulting mixture was cooled to 0 °C and NaNO<sub>2</sub> (0.895 g, 12.97 mmol) in H<sub>2</sub>O (5 mL) was added dropwise for 0.5 h. Reaction was stirred under ice-cooling for 1 h. Then CuBr (2.75 g, 19.26mmol) in 48% of HBr (5 mL) was added dropwise for 5 min. The mixture was stirred for 2 h at 70 °C. Upon completion, the pH was adjusted to 9-10 with saturated sodium carbonate solution. The reaction mixture was extracted with ethyl acetate (60 mL × 3), which was washed with water (30 mL × 3) and brine (30 mL × 3) successively, dried over NaSO<sub>4</sub>, filtered and concentrated in vacuo. The residue was

purified by silica gel column chromatography (n-hexane/ethyl acetate, 10/1, v/v) to afford title compound as a yellow solid. Yield: 50%. R<sub>f</sub>: 0.36 (n-hexane/ethyl acetate, 5/1, v/v). <sup>1</sup>H NMR (300 MHz, DMSO-*d*<sub>6</sub>) δ: 9.14 (s, 1H), 8.57 (s, 1H), 8.35 (d, *J* = 2.1 Hz, 1H), 8.04 (dd, *J* = 8.4, 2.1 Hz, 1H), 7.93 (d, *J* = 8.4 Hz, 1H), 2.58 (s, 3H). MS (m/z): [M+H]<sup>+</sup> 283.2.

**2-(4-Bromo-3-chlorophenyl)-6-methylpyridine (18b)** The preparation of compound **18b** was similar with that of compound **18a** to afford title compound as a yellow solid. Yield: 46%. R<sub>f</sub>: 0.36 (n-hexane/ethyl acetate, 2/1, v/v). <sup>1</sup>H NMR (300 MHz, DMSO-*d*<sub>6</sub>) δ: 8.31 (m, 1H), 7.98 (m, 1H), 7.84 (m, 3H), 7.27 (m, 1H), 2.54 (s, 3H). MS (m/z): [M+H]<sup>+</sup> 282.1.

**2-(3-Chloro-4-(4,4,5,5-tetramethyl-1,3,2-dioxaborolan-2-yl)phenyl)-6-methyl-pyrazine (19a)** To the solution of compound **18a** (2.00 g, 7.12 mmol) in dry dioxane (50 mL) were added Bis(pinacolato)diboron (2.17 g, 8.54 mmol), Potassium Acetate (2.09 g, 21.36 mmol) and Pd(dppf)Cl<sub>2</sub> (0.261 g, 0.356 mmol) under an argon atmosphere. Reaction mixture was stirred at 100 °C for 12 h. Upon completion, the solvent was removed in vacuo, and the residue was extracted with ethyl acetate (60 mL × 3). The combined organic extracts were washed with brine (30 mL × 3), dried over anhydrous Na<sub>2</sub>SO<sub>4</sub> and concentrated in vacuo. Black solid was afforded as the crude product which was used in next step.

**2-(3-Chloro-4-(4,4,5,5-tetramethyl-1,3,2-dioxaborolan-2-yl)phenyl)-6-methyl-pyridine (19b)** The preparation of compound **19b** was similar with that of compound **19a** to afford title compound as a yellow solid.

**Methyl 6-(2-chloro-4-(6-methylpyrazin-2-yl)phenyl)-1-(tetrahydro-2H-pyran-2-yl)-1H-indazole-3-carboxylate (20a)** To the solution of compound **19a** (1.90 g, 5.80 mmol) in dioxane (50 mL) and H<sub>2</sub>O (40 mL) were added compound **10** (1.97 g, 5.80 mmol), K<sub>2</sub>CO<sub>3</sub> (2.40 g, 17.4 mmol), Pd(dppf)Cl<sub>2</sub> (0.246 g, 0.290 mmol) under an argon atmosphere. Reaction mixture was stirred at 80 °C for 6 h. Upon completion, the solvent was removed in vacuo, and the residue was extracted with ethyl acetate (60 mL × 3). The combined organic extracts were washed with brine (30 mL × 3), dried over anhydrous Na<sub>2</sub>SO<sub>4</sub> and concentrated in vacuo. The residue was purified by silica gel column chromatography (n-hexane/ethyl acetate, 4/1, v/v) to afford title compound as a yellow solid. Yield: 90%. R<sub>f</sub>: 0.25 (n-hexane/ethyl acetate, 2/1, v/v). <sup>1</sup>H NMR (300 MHz, DMSO-*d*<sub>6</sub>) δ: 9.19 (s, 1H), 8.59 (s, 1H), 8.38 (s, 1H), 8.22 (m, 3H), 8.01 (s, 1H), 7.68 (m, 1H), 7.52 (m, 1H), 6.09 (m, 1H), 3.98 (s, 3H), 3.90 (m, 1H), 3.81 (m, 2H), 2.62 (s, 3H), 2.41 (m, 1H), 2.05 (m, 2H), 1.77 (m, 1H), 1.61 (m, 3H). MS (m/z): [M+H]<sup>+</sup> 463.3.

**Methyl 6-(2-chloro-4-(6-methylpyridin-2-yl)phenyl)-1-(tetrahydro-2H-pyran-2-yl)-1H-indazole-3-carboxylate (20b)** The preparation of compound **20b** was similar with that of compound **20a** to afford title compound as a yellow solid. Yield: 82%. R<sub>f</sub>: 0.21 (n-hexane/ethyl acetate, 1/1, v/v). <sup>1</sup>H NMR (300 MHz, DMSO-*d*<sub>6</sub>) δ: 8.32 (d, *J* = 1.7 Hz, 1H), 8.18 (d, *J* = 3.1 Hz,

1H), 8.15 (d,  $J = 2.3$  Hz, 1H), 8.00 (s, 1H), 7.90 (d,  $J = 7.8$  Hz, 1H), 7.82 (t,  $J = 7.7$  Hz, 1H), 7.62 (d,  $J = 8.0$  Hz, 1H), 7.49 (dd,  $J = 8.4, 1.3$  Hz, 1H), 7.29 (d,  $J = 7.5$  Hz, 1H), 6.09 (dd,  $J = 9.6, 2.3$  Hz, 1H), 3.98 (s, 3H), 3.90 (m, 1H), 3.81 (m, 1H), 2.58 (s, 3H), 2.41 (m, 1H), 2.04 (m, 2H), 1.74 (m, 1H), 1.60 (m, 2H). MS ( $m/z$ ):  $[M+H]^+$  462.4.

**6-(2-Chloro-4-(6-methylpyrazin-2-yl)phenyl)-1-(tetrahydro-2H-pyran-2-yl)-1H-indazole-3-carboxylic acid (21a)** To the solution of compound **20a** (1.00 g, 2.17 mmol) in MeOH (30 mL) and H<sub>2</sub>O (30 mL) were added NaOH (0.434 g, 10.85 mmol). Reaction mixture was stirred at 65 °C for 2 h. Upon completion, the solvent was removed in vacuo. The pH was adjusted to 9-10 with 2 M HCl. The aqueous phase was extracted with ethyl acetate (60 mL × 3). The combined organic extracts were washed with brine (30 mL × 3), dried over anhydrous Na<sub>2</sub>SO<sub>4</sub> and concentrated in vacuo. Yellow solid was afforded as the crude product which was used in next step.

**6-(2-Chloro-4-(6-methylpyridin-2-yl)phenyl)-1-(tetrahydro-2H-pyran-2-yl)-1H-indazole-3-carboxylic acid (21b)** The preparation of compound **21b** was similar with that of compound **21a** to afford title compound as the crude product which was used in next step.

**6-(2-Chloro-4-(6-methylpyrazin-2-yl)phenyl)-N-methyl-1-(tetrahydro-2H-pyran-2-yl)-1H-indazole-3-carboxamide (22a)** To the solution of compound **21a** (0.145 g, 0.324 mmol) in dry DMF (20 mL) were added HATU (0.246 g, 0.648 mmol), DIEA (0.125 g, 0.972 mmol) and 2 M CH<sub>3</sub>NH<sub>2</sub>-MeOH (0.5 mL, 32.2 mol). Reaction mixture was stirred at 25 °C for 12 h. Upon completion, the reaction mixture was quenched with ethyl acetate (30 mL), which was washed with water (20 mL × 3) and brine (20 mL × 3) successively, dried over Na<sub>2</sub>SO<sub>4</sub>, filtered and concentrated in vacuo. The residue was purified by silica gel column chromatography (n-hexane/ethyl acetate, 2/1, v/v) to afford title compound as a yellow solid. Yellow solid was afforded as the crude product which was used in next step.

**6-(2-Chloro-4-(6-methylpyridin-2-yl)phenyl)-N-methyl-1-(tetrahydro-2H-pyran-2-yl)-1H-indazole-3-carboxamide (22b)** The preparation of compound **22b** was similar with that of compound **22a** to afford title compound as the crude product which was used in next step.

**6-(2-Chloro-4-(6-methylpyrazin-2-yl)phenyl)-N-(cyclopropylmethyl)-1-(tetrahydro-2H-pyran-2-yl)-1H-indazole-3-carboxamide (22c)** The preparation of compound **22c** was similar with that of compound **22a** to afford title compound as the crude product which was used in next step.

**6-(2-Chloro-4-(6-methylpyridin-2-yl)phenyl)-N-(cyclopropylmethyl)-1-(tetrahydro-2H-pyran-2-yl)-1H-indazole-3-carboxamide (22d)** The preparation of compound **22d** was similar with that of compound **22a** to afford title compound as the crude product which was used in next step.

**6-(2-Chloro-4-(6-methylpyrazin-2-yl)phenyl)-N-methyl-1H-indazole-3-carboxamide (23a)** To

the solution of compound **22a** (0.120 g, 0.261 mmol) in MeOH (10 mL) and 6 M HCl (8 mL). The resulting mixture was heated to 65 °C for 12 h. Upon completion, the solvent was removed in vacuo. The pH was adjusted to 9-10 with saturated sodium carbonate solution. The aqueous phase was extracted with ethyl acetate (30 mL × 3). The combined organic extracts were washed with brine (20 mL × 3), dried over anhydrous Na<sub>2</sub>SO<sub>4</sub> and concentrated in vacuo. The residue was purified by silica gel column chromatography (DCM/MeOH, 100/1, v/v) to afford title compound as a yellow solid. Yield: 57%. mp: 266-271 °C. R<sub>f</sub>: 0.26 (DCM/MeOH, 50/1, v/v). <sup>1</sup>H NMR (300 MHz, DMSO-*d*<sub>6</sub>) δ: 13.75 (s, 1H), 9.18 (s, 1H), 8.58 (s, 1H), 8.43 (q, *J* = 4.6 Hz, 1H), 8.35 (d, *J* = 1.8 Hz, 1H), 8.27 (dd, *J* = 8.4, 0.9 Hz, 1H), 8.21 (dd, *J* = 8.1, 1.8 Hz, 1H), 7.70 (t, *J* = 1.2 Hz, 1H), 7.67 (d, *J* = 8.1 Hz, 1H), 7.36 (dd, *J* = 8.4, 1.4 Hz, 1H), 2.86 (d, *J* = 4.8 Hz, 3H), 2.61 (s, 3H). <sup>13</sup>C NMR (100 MHz, DMSO-*d*<sub>6</sub>) δ: 163.11, 153.66, 148.85, 144.19, 141.41, 141.34, 139.53, 139.00, 137.47, 136.87, 132.85, 132.81, 128.18, 126.02, 124.20, 121.88, 121.39, 111.61, 26.03, 21.80. HRMS-EI *m/z* [M+H]<sup>+</sup> calcd for C<sub>20</sub>H<sub>17</sub>ClN<sub>5</sub>O: 378.1091, found: 378.1116.

**6-(2-Chloro-4-(6-methylpyridin-2-yl)phenyl)-*N*-methyl-1*H*-indazole-3-carboxamide (23b)**

The preparation of compound **23b** was similar with that of compound **23a** to afford title compound as a white solid. Yield: 59%. mp: 284-288 °C. R<sub>f</sub>: 0.38 (DCM/MeOH, 50/1, v/v). <sup>1</sup>H NMR (300 MHz, DMSO-*d*<sub>6</sub>) δ: 13.77 (s, 1H), 8.42 (q, *J* = 4.7 Hz, 1H), 8.30 (d, *J* = 1.6 Hz, 1H), 8.27 (d, *J* = 8.5 Hz, 1H), 8.13 (dd, *J* = 8.1, 1.7 Hz, 1H), 7.88 (d, *J* = 7.8 Hz, 1H), 7.80 (t, *J* = 7.7 Hz, 1H), 7.69 (s, 1H), 7.60 (d, *J* = 8.1 Hz, 1H), 7.35 (d, *J* = 8.4 Hz, 1H), 7.27 (d, *J* = 7.4 Hz, 1H), 2.86 (d, *J* = 4.6 Hz, 3H), 2.57 (s, 3H). <sup>13</sup>C NMR (100 MHz, DMSO-*d*<sub>6</sub>) δ: 163.16, 158.50, 153.75, 141.45, 140.45, 140.22, 139.01, 138.13, 137.09, 132.59, 132.53, 128.02, 125.82, 124.28, 123.12, 121.85, 121.34, 118.05, 111.57, 26.04, 24.78. HRMS-EI *m/z* [M+H]<sup>+</sup> calcd for C<sub>21</sub>H<sub>18</sub>ClN<sub>4</sub>O: 377.1091, found: 377.1164.

**6-(2-Chloro-4-(6-methylpyrazin-2-yl)phenyl)-*N*-(cyclopropylmethyl)-1*H*-indazole-3-carboxamide (23c)**

The preparation of compound **23c** was similar with that of compound **23a** to afford title compound as a white solid. Yield: 51%. mp: 228-233 °C. R<sub>f</sub>: 0.28 (DCM/MeOH, 50/1, v/v). <sup>1</sup>H NMR (300 MHz, DMSO-*d*<sub>6</sub>) δ: 13.68 (s, 1H), 9.05 (s, 1H), 8.45 (s, 1H), 8.40 (t, *J* = 6.0 Hz, 1H), 8.22 (d, *J* = 1.8 Hz, 1H), 8.15 (d, *J* = 8.4 Hz, 1H), 8.08 (dd, *J* = 8.1, 1.8 Hz, 1H), 7.59 (s, 1H), 7.53 (d, *J* = 8.1 Hz, 1H), 7.23 (dd, *J* = 8.4, 1.4 Hz, 1H), 3.10 (t, *J* = 6.4 Hz, 2H), 2.48 (s, 3H), 0.99 (m, 1H), 0.33 (m, 2H), 0.18 (m, 2H). <sup>13</sup>C NMR (100 MHz, DMSO-*d*<sub>6</sub>) δ: 162.49, 153.66, 148.85, 144.19, 141.47, 141.33, 139.52, 139.00, 137.47, 136.89, 132.85, 132.81, 128.18, 126.02, 124.22, 121.91, 121.45, 111.64, 43.19, 21.80, 11.75, 3.77. HRMS-EI *m/z* [M+H]<sup>+</sup> calcd for C<sub>23</sub>H<sub>21</sub>ClN<sub>5</sub>O: 418.1356, found: 418.1429.

**6-(2-Chloro-4-(6-methylpyridin-2-yl)phenyl)-*N*-(cyclopropylmethyl)-1*H*-indazole-3-carboxamide (23d)**

The preparation of compound **23d** was similar with that of compound **23a** to afford

title compound as a white solid. Yield: 62%. mp: 217-222 °C. R<sub>f</sub>: 0.40 (DCM/MeOH, 50/1, v/v). <sup>1</sup>H NMR (300 MHz, DMSO-*d*<sub>6</sub>) δ: 13.80 (s, 1H), 8.49 (t, *J* = 6.0 Hz, 1H), 8.30 (d, *J* = 1.7 Hz, 1H), 8.27 (d, *J* = 8.4 Hz, 1H), 8.14 (dd, *J* = 8.1, 1.8 Hz, 1H), 7.88 (d, *J* = 7.8 Hz, 1H), 7.80 (t, *J* = 7.7 Hz, 1H), 7.70 (s, 1H), 7.61 (d, *J* = 8.0 Hz, 1H), 7.35 (dd, *J* = 8.4, 1.4 Hz, 1H), 7.27 (d, *J* = 7.4 Hz, 1H), 3.22 (t, *J* = 6.4 Hz, 2H), 2.57 (s, 3H), 1.11 (m, 1H), 0.44 (m, 2H), 0.29 (m, 2H). <sup>13</sup>C NMR (100 MHz, DMSO-*d*<sub>6</sub>) δ: 162.50, 158.52, 153.75, 141.51, 140.46, 140.23, 139.01, 138.18, 137.10, 132.63, 132.54, 128.03, 125.85, 124.31, 123.16, 121.87, 121.39, 118.08, 111.59, 43.18, 24.80, 11.75, 3.77. HRMS-EI *m/z* [M+H]<sup>+</sup> calcd for C<sub>24</sub>H<sub>22</sub>ClN<sub>4</sub>O: 417.1404, found: 417.1477.

**1-(4-Amino-3-chlorophenyl)pyridin-2(1H)-one (24a)** In a sealed tube, compound **15** (4.0 g, 19.4 mmol) was dissolved in anhydrous dioxane (50 mL), followed by the addition of 2-hydroxypyridine (2.77 g, 29.1 mmol), potassium phosphate (6.17 g, 29.13 mmol), cuprous iodide (0.742 g, 3.88 mmol) and N,N-Dimethylethylene-diamine (0.740 g, 7.77 mmol) under an argon atmosphere. Reaction was heated to 120 °C for 24 h. Upon completion, the solvent was removed in vacuo, and the residue was extracted with ethyl acetate (70 mL × 3). The combined organic extracts were washed with brine (30 mL × 3), dried over anhydrous Na<sub>2</sub>SO<sub>4</sub> and concentrated in vacuo. The residue was purified by silica gel column chromatography (n-hexane/ethyl acetate, 2/1, v/v) to afford title compound as a yellow solid. Yield: 90%. R<sub>f</sub>: 0.32 (n-hexane/ethyl acetate, 1/1, v/v). <sup>1</sup>H NMR (300 MHz, DMSO-*d*<sub>6</sub>) δ: 7.56 (dd, *J* = 6.9, 2.1 Hz, 1H), 7.45 (m, 1H), 7.26 (d, *J* = 2.4 Hz, 1H), 7.04 (dd, *J* = 8.6, 2.4 Hz, 1H), 6.86 (d, *J* = 8.6 Hz, 1H), 6.44 (d, *J* = 8.6 Hz, 1H), 6.25 (m, 1H), 5.61 (s, 2H). MS (*m/z*): [M+H]<sup>+</sup> 221.1.

**1-(4-Amino-3-chlorophenyl)-3-methylpyridin-2(1H)-one (24b)** The preparation of compound **24b** was similar with that of compound **24a** to afford title compound as a yellow solid. Yield: 91%. R<sub>f</sub>: 0.38 (n-hexane/ethyl acetate, 1/1, v/v). <sup>1</sup>H NMR (300 MHz, DMSO-*d*<sub>6</sub>) δ: 7.43 (dd, *J* = 6.8, 2.1 Hz, 1H), 7.35 (m, 1H), 7.24 (d, *J* = 2.4 Hz, 1H), 7.02 (dd, *J* = 8.6, 2.4 Hz, 1H), 6.84 (d, *J* = 8.6 Hz, 1H), 6.17 (t, *J* = 6.8 Hz, 1H), 5.61 (s, 2H), 2.01 (s, 3H). MS (*m/z*): [M+H]<sup>+</sup> 235.1.

**1-(4-Bromo-3-chlorophenyl)pyridin-2(1H)-one (25a)** To a stirring solution of 48% of HBr (10 mL) and H<sub>2</sub>O (10 mL) were added compound **24a** (3.00 g, 12.82 mmol). The resulting mixture was cooled to 0 °C and NaNO<sub>2</sub> (0.855 g, 12.82 mmol) in H<sub>2</sub>O (5 mL) was added dropwise for 0.5 h. Reaction was stirred under ice-cooling for 1 h. Then CuBr (2.75 g, 19.23 mmol) in 48% of HBr (10 mL) was added dropwise for 5 min. The mixture was stirred for 4 h at 80 °C. Upon completion, the reaction mixture was extracted with ethyl acetate (80 mL × 3), which was washed with water (40 mL × 3) and brine (40 mL × 3) successively, dried over Na<sub>2</sub>SO<sub>4</sub>, filtered and concentrated in vacuo. The residue was purified by silica gel column chromatography (n-hexane/ethyl acetate, 5/1, v/v) to afford title compound as a yellow solid. Yield: 90%. R<sub>f</sub>: 0.26 (n-hexane/ethyl acetate, 4/1, v/v). <sup>1</sup>H NMR (300 MHz, DMSO-*d*<sub>6</sub>) δ: 7.91 (d, *J* = 8.5 Hz, 1H),

7.79 (d,  $J = 2.5$  Hz, 1H), 7.67 (m, 1H), 7.52 (m, 1H), 7.37 (dd,  $J = 8.6, 2.5$  Hz, 1H), 6.50 (m, 1H), 6.34 (m, 1H). MS (m/z):  $[M+H]^+$  284.0.

**1-(4-Bromo-3-chlorophenyl)-3-methylpyridin-2(1H)-one (25b)** The preparation of compound **25b** was similar with that of compound **25a** to afford title compound as a yellow solid. Yield: 86%.  $R_f$ : 0.30 (n-hexane/ethyl acetate, 4/1, v/v).  $^1H$  NMR (300 MHz, DMSO- $d_6$ )  $\delta$ : 7.90 (d,  $J = 8.6$  Hz, 1H), 7.78 (d,  $J = 2.4$  Hz, 1H), 7.53 (dd,  $J = 7.2, 1.6$  Hz, 1H), 7.40 (m, 1H), 7.36 (dd,  $J = 8.5, 2.5$  Hz, 1H), 6.25 (t,  $J = 6.8$  Hz, 1H), 2.04 (s, 3H). MS (m/z):  $[M+H]^+$  298.0.

**1-(3-Chloro-4-(4,4,5,5-tetramethyl-1,3,2-dioxaborolan-2-yl)phenyl)pyridin-2(1H)-one (26a)** To the solution of compound **25a** (2.00 g, 6.73 mmol) in dry dioxane (50 mL) were added Bis(pinacolato)diboron (2.57 g, 10.10 mmol), Potassium Acetate (1.97 g, 20.13 mmol) and Pd(dppf)Cl<sub>2</sub> (0.246 g, 0.336 mmol) under an argon atmosphere. Reaction mixture was stirred at 100 °C for 12 h. Upon completion, the solvent was removed in vacuo, and the residue was extracted with ethyl acetate (60 mL  $\times$  3). The combined organic extracts were washed with brine (30 mL  $\times$  3), dried over anhydrous Na<sub>2</sub>SO<sub>4</sub> and concentrated in vacuo. Black solid was afforded as the crude product which was used in next step.

**1-(3-Chloro-4-(4,4,5,5-tetramethyl-1,3,2-dioxaborolan-2-yl)phenyl)-3-methyl-pyridin-2(1H)-one (26b)** The preparation of compound **26b** was similar with that of compound **26a** to afford title compound as a black solid.

**Methyl 6-(2-chloro-4-(2-oxopyridin-1(2H)-yl)phenyl)-1-(tetrahydro-2H-pyran-2-yl)-1H-indazole-3-carboxylate (27a)** To the solution of compound **26a** (2.00 g, 5.80 mmol) in dioxane (50 mL) and H<sub>2</sub>O (40 mL) were added compound **9** (1.97 g, 5.80 mmol), K<sub>2</sub>CO<sub>3</sub> (2.40 g, 17.4 mmol), Pd(dppf)Cl<sub>2</sub> (0.246 g, 0.290 mmol) under an argon atmosphere. Reaction mixture was stirred at 80 °C for 6 h. Upon completion, the solvent was removed in vacuo, and the residue was extracted with ethyl acetate (60 mL  $\times$  3). The combined organic extracts were washed with brine (30 mL  $\times$  3), dried over anhydrous Na<sub>2</sub>SO<sub>4</sub> and concentrated in vacuo. The residue was purified by silica gel column chromatography (n-hexane/ethyl acetate, 2/1, v/v) to afford title compound as a yellow solid. Yield: 84%.  $R_f$ : 0.32 (n-hexane/ethyl acetate, 1/1, v/v).  $^1H$  NMR (300 MHz, DMSO- $d_6$ )  $\delta$ : 8.09 (dd,  $J = 8.5, 4.0$  Hz, 1H), 7.91 (d,  $J = 4.0$  Hz, 1H), 7.74 – 7.34 (m, 6H), 6.44 (dd,  $J = 9.3, 3.9$  Hz, 1H), 6.28 (q,  $J = 6.7, 4.9$  Hz, 1H), 5.99 (dd,  $J = 8.2, 3.7$  Hz, 1H), 3.88 (s, 3H), 3.83 – 3.66 (m, 2H), 2.30 (m, 1H), 2.01 – 1.87 (m, 2H), 1.66 (m, 2H), 1.51 (m, 2H). MS (m/z):  $[M+H]^+$  464.3.

**Methyl 6-(2-chloro-4-(3-methyl-2-oxopyridin-1(2H)-yl)phenyl)-1-(tetrahydro-2H-pyran-yl)-1H-indazole-3-carboxylate (27b)**. The preparation of compound **27b** was similar with that of compound **27a** to afford title compound as a yellow solid. Yield: 87%.  $R_f$ : 0.36 (n-hexane/ethyl acetate, 1/1, v/v).  $^1H$  NMR (300 MHz, DMSO- $d_6$ )  $\delta$ : 8.20 (m, 1H), 8.00 (s, 1H), 7.76 (m, 1H), 7.56 (m, 5H), 6.30 (m, 1H), 6.09 (d,  $J = 9.1$  Hz, 1H), 3.96 (s, 3H), 3.84 (m, 2H), 2.41 (m, 1H),

2.07 (s, 3H), 2.03 (m, 2H), 1.74 (m, 1H), 1.60 (m, 2H). MS (m/z): [M+H]<sup>+</sup> 478.2.

**6-(2-Chloro-4-(2-oxopyridin-1(2H)-yl)phenyl)-1-(tetrahydro-2H-pyran-2-yl)-1H-indazole-3-carboxylic acid (28a)** To the solution of compound **27a** (1.00 g, 2.09 mmol) in MeOH (30 mL) and H<sub>2</sub>O (30 mL) were added NaOH (0.418 g, 10.46 mmol). Reaction mixture was stirred at 65 °C for 2 h. Upon completion, the solvent was removed in vacuo. The pH was adjusted to 9-10 with 2 M HCl. The aqueous phase was extracted with ethyl acetate (60 mL × 3). The combined organic extracts were washed with brine (30 mL × 3), dried over anhydrous Na<sub>2</sub>SO<sub>4</sub> and concentrated in vacuo. Yellow solid was afforded as the crude product which was used in next step.

**6-(2-Chloro-4-(3-methyl-2-oxopyridin-1(2H)-yl)phenyl)-1-(tetrahydro-2H-pyran-2-yl)-1H-indazole-3-carboxylic acid (28b)** The preparation of compound **28b** was similar with that of compound **28a** to afford title compound as a yellow solid. Yellow solid was afforded as the crude product which was used in next step.

**6-(2-Chloro-4-(3-methyl-2-oxopyridin-1(2H)-yl)phenyl)-N-methyl-1-(tetrahydro-2H-pyran-2-yl)-1H-indazole-3-carboxamide (29a)** To the solution of compound **28b** (0.150 g, 0.324 mmol) in dry DMF (20 mL) were added HATU (0.246 g, 0.648 mmol), DIEA (0.125 g, 0.972 mmol) and 2 M CH<sub>3</sub>NH<sub>2</sub>-MeOH (0.5 mL, 32.2 mmol). Reaction mixture was stirred at 25 °C for 12 h. Upon completion, the reaction mixture was quenched with ethyl acetate (30 mL), which was washed with water (20 mL × 3) and brine (20 mL × 3) successively, dried over Na<sub>2</sub>SO<sub>4</sub>, filtered and concentrated in vacuo. The residue was purified by silica gel column chromatography (n-hexane/ethyl acetate, 2/1, v/v) to afford title compound as a yellow solid. Yellow solid was afforded as the crude product which was used in next step.

**6-(2-Chloro-4-(2-oxopyridin-1(2H)-yl)phenyl)-N-methyl-1-(tetrahydro-2H-pyran-2-yl)-1H-indazole-3-carboxamide (29b)** The preparation of compound **29b** was similar with that of compound **29a** to afford title compound as the crude product which was used in next step.

**6-(2-Chloro-4-(3-methyl-2-oxopyridin-1(2H)-yl)phenyl)-N-(cyclopropylmethyl)-1-(tetrahydro-2H-pyran-2-yl)-1H-indazole-3-carboxamide (29c)** The preparation of compound **29c** was similar with that of compound **29a** to afford title compound as the crude product which was used in next step.

**6-(2-Chloro-4-(2-oxopyridin-1(2H)-yl)phenyl)-N-(cyclopropylmethyl)-1-(tetrahydro-2H-pyran-2-yl)-1H-indazole-3-carboxamide (29d)** The preparation of compound **29d** was similar with that of compound **29a** to afford title compound as the crude product which was used in next step.

**6-(2-Chloro-4-(3-methyl-2-oxopyridin-1(2H)-yl)phenyl)-N-ethyl-1-(tetrahydro-2H-pyran-2-yl)-1H-indazole-3-carboxamide (29e)** The preparation of compound **29e** was similar with that of compound **29a** to afford title compound as the crude product which was used in next step.

**6-(2-Chloro-4-(3-methyl-2-oxopyridin-1(2H)-yl)phenyl)-N-(2-hydroxyethyl)-1-(tetrahydro-2H-pyran-2-yl)-1H-indazole-3-carboxamide (29f)** The preparation of compound **29f** was similar with that of compound **29a** to afford title compound as the crude product which was used in next step.

**6-(2-Chloro-4-(3-methyl-2-oxopyridin-1(2H)-yl)phenyl)-N-(2-methoxyethyl)-1-(tetrahydro-2H-pyran-2-yl)-1H-indazole-3-carboxamide (29g)** The preparation of compound **29g** was similar with that of compound **29a** to afford title compound as the crude product which was used in next step.

**1-(3-Chloro-4-(3-(pyrrolidine-1-carbonyl)-1-(tetrahydro-2H-pyran-2-yl)-1H-indazol-6-yl)phenyl)-3-methylpyridin-2(1H)-one (29h)** The preparation of compound **29h** was similar with that of compound **29a** to afford title compound as the crude product which was used in next step.

**1-(3-Chloro-4-(3-(morpholine-4-carbonyl)-1-(tetrahydro-2H-pyran-2-yl)-1H-indazol-6-yl)phenyl)-3-methylpyridin-2(1H)-one (29i)** The preparation of compound **29i** was similar with that of compound **29a** to afford title compound as the crude product which was used in next step.

**N-benzyl-6-(2-chloro-4-(3-methyl-2-oxopyridin-1(2H)-yl)phenyl)-1-(tetrahydro-2H-pyran-2-yl)-1H-indazole-3-carboxamide (29j)** The preparation of compound **29j** was similar with that of compound **29a** to afford title compound as the crude product which was used in next step.

**6-(2-Chloro-4-(3-methyl-2-oxopyridin-1(2H)-yl)phenyl)-N-(pyridin-4-yl)-1-(tetrahydro-2H-pyran-2-yl)-1H-indazole-3-carboxamide (29k)** The preparation of compound **29k** was similar with that of compound **29a** to afford title compound as the crude product which was used in next step.

**6-(2-Chloro-4-(3-methyl-2-oxopyridin-1(2H)-yl)phenyl)-N-(pyridin-4-ylmethyl)-1-(tetrahydro-2H-pyran-2-yl)-1H-indazole-3-carboxamide (29l)** The preparation of compound **29l** was similar with that of compound **29a** to afford title compound as the crude product which was used in next step.

**6-(2-Chloro-4-(3-methyl-2-oxopyridin-1(2H)-yl)phenyl)-N-(2-(pyridin-4-yl)ethyl)-1-(tetrahydro-2H-pyran-2-yl)-1H-indazole-3-carboxamide (29m)** The preparation of compound **29m** was similar with that of compound **29a** to afford title compound as the crude product which was used in next step.

**6-(2-Chloro-4-(3-methyl-2-oxopyridin-1(2H)-yl)phenyl)-1-(tetrahydro-2H-pyran-2-yl)-N-(tetrahydro-2H-pyran-4-yl)-1H-indazole-3-carboxamide (29n)** The preparation of compound **29n** was similar with that of compound **29a** to afford title compound as the crude product which was used in next step.

**6-(2-Chloro-4-(3-methyl-2-oxopyridin-1(2H)-yl)phenyl)-N-(1-methylpiperidin-4-yl)-1-(tetrahydro-2H-pyran-2-yl)-1H-indazole-3-carboxamide (29o)** The preparation of compound **29o**

was similar with that of compound **29a** to afford title compound as the crude product which was used in next step.

**6-(2-Chloro-4-(3-methyl-2-oxopyridin-1(2H)-yl)phenyl)-1-(tetrahydro-2H-pyran-2-yl)-N-((tetrahydro-2H-pyran-4-yl)methyl)-1H-indazole-3-carboxamide (29p)** The preparation of compound **29p** was similar with that of compound **29a** to afford title compound as the crude product which was used in next step.

**6-(2-Chloro-4-(3-methyl-2-oxopyridin-1(2H)-yl)phenyl)-N-((1-methylpiperidin-4-yl)methyl)-1-(tetrahydro-2H-pyran-2-yl)-1H-indazole-3-carboxamide (29q)** The preparation of compound **29q** was similar with that of compound **29a** to afford title compound as the crude product which was used in next step.

**6-(2-Chloro-4-(3-methyl-2-oxopyridin-1(2H)-yl)phenyl)-N-methyl-1H-indazole-3-carboxamide (30a)** To the solution of compound **29a** (0.120 g, 0.259 mmol) in MeOH (10 mL) and 6 M HCl (8 mL). The resulting mixture was heated to 65 °C for 12 h. Upon completion, the solvent was removed in vacuo. The pH was adjusted to 9-10 with saturated sodium carbonate solution. The aqueous phase was extracted with ethyl acetate (30 mL × 3). The combined organic extracts were washed with brine (20 mL × 3), dried over anhydrous Na<sub>2</sub>SO<sub>4</sub> and concentrated in vacuo. The residue was purified by silica gel column chromatography (DCM/MeOH, 100/1) to afford title compound as a white solid. Yield: 61%. mp: 290-295 °C. R<sub>f</sub>: 0.34 (DCM/MeOH, 50/1, v/v). <sup>1</sup>H NMR (300 MHz, DMSO-*d*<sub>6</sub>) δ: 13.75 (s, 1H), 8.45 (q, *J* = 4.5 Hz, 1H), 8.27 (dd, *J* = 8.4, 0.8 Hz, 1H), 7.74 (d, *J* = 2.1 Hz, 1H), 7.68 (t, *J* = 1.2 Hz, 1H), 7.64 (d, *J* = 8.3 Hz, 1H), 7.60 (m, 1H), 7.51 (dd, *J* = 8.2, 2.1 Hz, 1H), 7.43 (m, 1H), 7.33 (dd, *J* = 8.4, 1.4 Hz, 1H), 6.29 (t, *J* = 6.8 Hz, 1H), 2.85 (d, *J* = 4.7 Hz, 3H), 2.07 (s, 3H). <sup>13</sup>C NMR (100 MHz, DMSO-*d*<sub>6</sub>) δ: 163.13, 162.13, 141.76, 141.45, 139.96, 138.99, 138.13, 136.68, 136.52, 132.49, 131.97, 129.59, 128.75, 126.49, 124.20, 121.95, 121.39, 111.67, 106.00, 26.03, 17.48. HRMS-EI *m/z* [M+H]<sup>+</sup> calcd for C<sub>21</sub>H<sub>18</sub>ClN<sub>4</sub>O<sub>2</sub>: 392.1040, found: 392.1113.

**6-(2-Chloro-4-(2-oxopyridin-1(2H)-yl)phenyl)-N-methyl-1H-indazole-3-carboxamide (30b)** The preparation of compound **30b** was similar with that of compound **30a** to afford title compound as a white solid. Yield: 58%. mp: 286-291 °C. R<sub>f</sub>: 0.32 (DCM/MeOH, 50/1, v/v). <sup>1</sup>H NMR (300 MHz, DMSO-*d*<sub>6</sub>) δ: 13.76 (s, 1H), 8.46 (q, *J* = 4.7 Hz, 1H), 8.30 (d, *J* = 8.4 Hz, 1H), 7.75 (m, 2H), 7.71 (s, 1H), 7.65 (d, *J* = 8.2 Hz, 1H), 7.55 (m, 2H), 7.35 (dd, *J* = 8.4, 1.4 Hz, 1H), 6.56 (d, *J* = 9.1 Hz, 1H), 6.38 (m, 1H), 2.88 (d, *J* = 4.7 Hz, 3H). <sup>13</sup>C NMR (100 MHz, DMSO-*d*<sub>6</sub>) δ: 163.16, 161.65, 141.42, 141.38, 140.08, 139.19, 139.01, 136.68, 132.52, 132.03, 128.66, 126.43, 124.21, 121.96, 121.40, 121.04, 111.65, 106.42, 26.04. HRMS-EI *m/z* [M+H]<sup>+</sup> calcd for C<sub>20</sub>H<sub>16</sub>ClN<sub>4</sub>O<sub>2</sub>: 379.0884, found: 379.0956.

**6-(2-Chloro-4-(3-methyl-2-oxopyridin-1(2H)-yl)phenyl)-N-(cyclopropylmethyl)-1H-indazole-**

**3-carboxamide (30c)** The preparation of compound **30c** was similar with that of compound **30a** to afford title compound as a white solid. Yield: 66%. mp: 284-289 °C. R<sub>f</sub>: 0.38 (DCM/MeOH, 50/1, v/v). <sup>1</sup>H NMR (300 MHz, DMSO-*d*<sub>6</sub>) δ: 13.73 (s, 1H), 8.49 (d, *J* = 6.3 Hz, 1H), 8.27 (d, *J* = 8.5 Hz, 1H), 7.79 – 7.57 (m, 4H), 7.51 (d, *J* = 7.8 Hz, 1H), 7.44 (d, *J* = 6.4 Hz, 1H), 7.34 (d, *J* = 8.4 Hz, 1H), 6.29 (t, *J* = 6.8 Hz, 1H), 3.21 (t, *J* = 6.6 Hz, 2H), 2.07 (s, 3H), 1.11 (m, 1H), 0.45 (m, 2H), 0.28 (m, 2H). <sup>13</sup>C NMR (100 MHz, DMSO-*d*<sub>6</sub>) δ: 162.53, 162.16, 141.77, 141.48, 139.97, 138.98, 138.19, 136.72, 136.53, 132.51, 131.97, 129.59, 128.74, 126.51, 124.23, 121.96, 121.42, 111.68, 106.06, 43.18, 17.46, 11.72, 3.75. HRMS-EI *m/z* [M+H]<sup>+</sup> calcd for C<sub>24</sub>H<sub>22</sub>ClN<sub>4</sub>O<sub>2</sub>: 433.1353, found: 433.1426.

**6-(2-Chloro-4-(2-oxopyridin-1(2*H*)-yl)phenyl)-*N*-(cyclopropylmethyl)-1*H*-indazole-3-carboxamide (30d)** The preparation of compound **30d** was similar with that of compound **30a** to afford title compound as a white solid. Yield: 57%. mp: 288-292 °C. R<sub>f</sub>: 0.36 (DCM/MeOH, 50/1, v/v). <sup>1</sup>H NMR (300 MHz, DMSO-*d*<sub>6</sub>) δ: 13.76 (s, 1H), 8.50 (t, *J* = 6.0 Hz, 1H), 8.27 (d, *J* = 8.4 Hz, 1H), 7.74 (q, *J* = 3.3 Hz, 2H), 7.69 (s, 1H), 7.64 (d, *J* = 8.2 Hz, 1H), 7.53 (m, 2H), 7.33 (dd, *J* = 8.4, 1.4 Hz, 1H), 6.54 (m, 1H), 6.37 (m, 1H), 3.21 (t, *J* = 6.4 Hz, 2H), 1.10 (m, 1H), 0.44 (m, 2H), 0.29 (m, 2H). <sup>13</sup>C NMR (100 MHz, DMSO-*d*<sub>6</sub>) δ: 162.51, 161.63, 141.48, 141.40, 140.08, 139.21, 139.00, 136.69, 132.53, 132.03, 128.67, 126.45, 124.21, 121.97, 121.45, 121.05, 111.67, 106.41, 43.19, 11.73, 3.76. HRMS-EI *m/z* [M+H]<sup>+</sup> calcd for C<sub>23</sub>H<sub>20</sub>ClN<sub>4</sub>O<sub>2</sub>: 419.1197, found: 419.1270.

**6-(2-Chloro-4-(3-methyl-2-oxopyridin-1(2*H*)-yl)phenyl)-*N*-ethyl-1*H*-indazole-3-carboxamide (30e)** The preparation of compound **30e** was similar with that of compound **30a** to afford title compound as a white solid. Yield: 68%. mp: 270-275 °C. R<sub>f</sub>: 0.36 (DCM/MeOH, 50/1, v/v). <sup>1</sup>H NMR (300 MHz, DMSO-*d*<sub>6</sub>) δ: 13.73 (s, 1H), 8.49 (t, *J* = 5.9 Hz, 1H), 8.26 (d, *J* = 8.4 Hz, 1H), 7.74 (d, *J* = 2.1 Hz, 1H), 7.68 (s, 1H), 7.67 – 7.57 (m, 2H), 7.51 (dd, *J* = 8.2, 2.2 Hz, 1H), 7.46 – 7.41 (m, 1H), 7.33 (dd, *J* = 8.4, 1.4 Hz, 1H), 6.29 (t, *J* = 6.8 Hz, 1H), 3.35 (m, 9H), 1.16 (t, *J* = 7.1 Hz, 3H). <sup>13</sup>C NMR (100 MHz, DMSO-*d*<sub>6</sub>) δ: 162.38, 162.13, 141.77, 141.44, 139.96, 139.06, 138.15, 136.68, 136.56, 132.50, 131.97, 129.58, 128.76, 126.52, 124.20, 121.98, 121.43, 111.65, 106.00, 33.70, 17.49, 15.52. HRMS-EI *m/z* [M+H]<sup>+</sup> calcd for C<sub>22</sub>H<sub>20</sub>ClN<sub>4</sub>O<sub>2</sub>: 407.1197, found: 407.1269.

**6-(2-Chloro-4-(3-methyl-2-oxopyridin-1(2*H*)-yl)phenyl)-*N*-(2-hydroxyethyl)-1*H*-indazole-3-carboxamide (30f)** The preparation of compound **30f** was similar with that of compound **30a** to afford title compound as a white solid. Yield: 46%. mp: 282-286 °C. R<sub>f</sub>: 0.16 (DCM/MeOH, 50/1, v/v). <sup>1</sup>H NMR (300 MHz, DMSO-*d*<sub>6</sub>) δ: 13.74 (s, 1H), 8.33 – 8.22 (m, 2H), 7.74 (d, *J* = 2.1 Hz, 1H), 7.69 (d, *J* = 1.1 Hz, 1H), 7.65 (d, *J* = 8.2 Hz, 1H), 7.61 (dd, *J* = 7.0, 2.0 Hz, 1H), 7.51 (dd, *J* = 8.2, 2.1 Hz, 1H), 7.43 (dt, *J* = 6.6, 1.6 Hz, 1H), 7.34 (dd, *J* = 8.4, 1.4 Hz, 1H), 6.29 (t, *J* = 6.8 Hz, 1H), 4.81 (t, *J* = 5.5 Hz, 1H), 3.57 (q, *J* = 6.0 Hz, 2H), 3.42 (q, *J* = 6.1 Hz, 2H), 2.07 (s, 3H). <sup>13</sup>C

NMR (100 MHz, DMSO- $d_6$ )  $\delta$ : 162.68, 162.14, 141.77, 141.47, 139.93, 138.83, 138.16, 136.73, 136.55, 132.51, 131.96, 129.58, 128.76, 126.52, 124.30, 121.92, 121.39, 111.70, 106.02, 60.34, 41.67, 17.49. HRMS-EI  $m/z$   $[M+H]^+$  calcd for  $C_{22}H_{20}ClN_4O_3$ : 423.1146, found: 423.1219.

**6-(2-Chloro-4-(3-methyl-2-oxopyridin-1(2H)-yl)phenyl)-N-(2-methoxyethyl)-1H-indazole-3-carboxamide (30g)** The preparation of compound **30g** was similar with that of compound **30a** to afford title compound as a white solid. Yield: 67%. mp: 226-231 °C.  $R_f$ : 0.28 (DCM/MeOH, 50/1, v/v).  $^1H$  NMR (300 MHz, DMSO- $d_6$ )  $\delta$ : 13.76 (s, 1H), 8.34 (m, 1H), 8.26 (dd,  $J = 8.5, 0.8$  Hz, 1H), 7.74 (d,  $J = 2.1$  Hz, 1H), 7.69 (t,  $J = 1.1$  Hz, 1H), 7.64 (d,  $J = 8.2$  Hz, 1H), 7.61 (dd,  $J = 7.3, 1.7$  Hz, 1H), 7.51 (dd,  $J = 8.2, 2.1$  Hz, 1H), 7.43 (m, 1H), 7.34 (dd,  $J = 8.4, 1.4$  Hz, 1H), 6.29 (t,  $J = 6.8$  Hz, 1H), 3.51 (m, 4H), 3.30 (s, 3H), 2.07 (s, 3H).  $^{13}C$  NMR (100 MHz, DMSO- $d_6$ )  $\delta$ : 162.64, 162.12, 141.78, 141.47, 139.92, 138.76, 138.12, 136.73, 136.54, 132.49, 131.97, 129.59, 128.76, 126.51, 124.31, 121.90, 121.40, 111.72, 105.98, 70.96, 58.37, 38.46, 17.49. HRMS-EI  $m/z$   $[M+H]^+$  calcd for  $C_{23}H_{22}ClN_4O_3$ : 437.1302, found: 437.1375.

**1-(3-Chloro-4-(3-(pyrrolidine-1-carbonyl)-1H-indazol-6-yl)phenyl)-3-methyl-pyridin-2(1H)-one (30h)** The preparation of compound **30h** was similar with that of compound **30a** to afford title compound as a white solid. Yield: 68%. mp: 285-290 °C.  $R_f$ : 0.56 (DCM/MeOH, 50/1, v/v).  $^1H$  NMR (300 MHz, DMSO- $d_6$ )  $\delta$ : 13.68 (s, 1H), 8.24 (d,  $J = 8.4$  Hz, 1H), 7.73 (d,  $J = 2.1$  Hz, 1H), 7.67 (t,  $J = 1.2$  Hz, 1H), 7.64 (d,  $J = 8.3$  Hz, 1H), 7.62 – 7.59 (m, 1H), 7.51 (dd,  $J = 8.2, 2.1$  Hz, 1H), 7.43 (m, 1H), 7.31 (dd,  $J = 8.4, 1.5$  Hz, 1H), 6.29 (t,  $J = 6.8$  Hz, 1H), 3.97 (t,  $J = 6.5$  Hz, 2H), 3.60 (t,  $J = 6.6$  Hz, 2H), 2.07 (s, 3H), 2.02 – 1.79 (m, 4H). HRMS-EI  $m/z$   $[M+H]^+$  calcd for  $C_{24}H_{22}ClN_4O_2$ : 433.1353, found: 433.1426.

**1-(3-Chloro-4-(3-(morpholine-4-carbonyl)-1H-indazol-6-yl)phenyl)-3-methyl-pyridin-2(1H)-one (30i)** The preparation of compound **30i** was similar with that of compound **30a** to afford title compound as a white solid. Yield: 69%. mp: 249-254 °C.  $R_f$ : 0.38 (DCM/MeOH, 50/1, v/v).  $^1H$  NMR (300 MHz, DMSO- $d_6$ )  $\delta$ : 13.73 (s, 1H), 8.09 (d,  $J = 8.4$  Hz, 1H), 7.74 (d,  $J = 2.1$  Hz, 1H), 7.69 (t,  $J = 1.1$  Hz, 1H), 7.63 (d,  $J = 8.3$  Hz, 1H), 7.59 (m, 1H), 7.51 (dd,  $J = 8.2, 2.1$  Hz, 1H), 7.46 – 7.40 (m, 1H), 7.32 (dd,  $J = 8.4, 1.4$  Hz, 1H), 6.29 (t,  $J = 6.8$  Hz, 1H), 4.08 (m, 2H), 3.72 (m, 6H), 2.07 (s, 3H). HRMS-EI  $m/z$   $[M+H]^+$  calcd for  $C_{24}H_{22}ClN_4O_3$ : 449.1302, found: 449.1375.

**N-benzyl-6-(2-chloro-4-(3-methyl-2-oxopyridin-1(2H)-yl)phenyl)-1H-indazole-3-carboxamide (30j)** The preparation of compound **30j** was similar with that of compound **30a** to afford title compound as a white solid. Yield: 71%. mp: 269-274 °C.  $R_f$ : 0.52 (DCM/MeOH, 50/1, v/v).  $^1H$  NMR (300 MHz, DMSO- $d_6$ )  $\delta$ : 13.69 (s, 1H), 8.99 (t,  $J = 6.3$  Hz, 1H), 8.27 (dd,  $J = 8.3, 0.9$  Hz, 1H), 7.73 (d,  $J = 2.1$  Hz, 1H), 7.69 (t,  $J = 1.2$  Hz, 1H), 7.64 (d,  $J = 8.2$  Hz, 1H), 7.62 – 7.57 (m, 1H), 7.51 (dd,  $J = 8.2, 2.1$  Hz, 1H), 7.45 – 7.41 (m, 1H), 7.41 – 7.29 (m, 5H), 7.27 – 7.20 (m, 1H), 6.28 (t,  $J = 6.8$  Hz, 1H), 4.54 (d,  $J = 6.3$  Hz, 2H), 2.07 (s, 3H).  $^{13}C$  NMR (100 MHz, DMSO- $d_6$ )  $\delta$ :

162.66, 162.13, 141.79, 141.49, 140.42, 139.94, 138.82, 138.13, 136.76, 136.55, 132.50, 131.97, 129.59, 128.73, 127.78, 127.15, 126.52, 124.33, 121.90, 121.50, 111.71, 105.99, 42.38, 17.48. HRMS-EI  $m/z$   $[M+H]^+$  calcd for  $C_{27}H_{22}ClN_4O_2$ : 469.1353, found: 469.1426.

**6-(2-Chloro-4-(3-methyl-2-oxopyridin-1(2H)-yl)phenyl)-N-(pyridin-4-yl)-1H-indazole-3-carboxamide (30k)** The preparation of compound **30k** was similar with that of compound **30a** to afford title compound as a white solid. Yield: 67%. mp: 296-299 °C.  $R_f$ : 0.23 (DCM/MeOH, 50/1, v/v).  $^1H$  NMR (300 MHz, DMSO- $d_6$ )  $\delta$ : 14.10 (s, 1H), 10.82 (s, 1H), 8.53 – 8.46 (m, 2H), 8.32 (d,  $J$  = 8.4 Hz, 1H), 7.99 – 7.94 (m, 2H), 7.77 (d,  $J$  = 1.3 Hz, 1H), 7.75 (d,  $J$  = 2.1 Hz, 1H), 7.67 (d,  $J$  = 8.2 Hz, 1H), 7.61 (dd,  $J$  = 7.1, 2.0 Hz, 1H), 7.53 (dd,  $J$  = 8.2, 2.1 Hz, 1H), 7.43 (m, 2H), 6.30 (t,  $J$  = 6.8 Hz, 1H), 2.08 (s, 3H).  $^{13}C$  NMR (100 MHz, DMSO- $d_6$ )  $\delta$ : 162.17, 162.13, 150.68, 146.20, 141.89, 141.74, 139.78, 138.26, 138.15, 137.16, 136.56, 132.52, 131.99, 129.59, 128.80, 126.58, 125.02, 121.79, 121.67, 114.53, 112.04, 106.00, 17.48. HRMS-EI  $m/z$   $[M+H]^+$  calcd for  $C_{25}H_{19}ClN_5O_2$ : 456.1149, found: 456.1222.

**6-(2-Chloro-4-(3-methyl-2-oxopyridin-1(2H)-yl)phenyl)-N-(pyridin-4-ylmethyl)-1H-indazole-3-carboxamide (30l)** The preparation of compound **30l** was similar with that of compound **30a** to afford title compound as a white solid. Yield: 72%. mp: 144-146 °C.  $R_f$ : 0.25 (DCM/MeOH, 50/1, v/v).  $^1H$  NMR (300 MHz, DMSO- $d_6$ )  $\delta$ : 13.88 (s, 1H), 9.19 (t,  $J$  = 6.3 Hz, 1H), 8.53 (d,  $J$  = 1.6 Hz, 1H), 8.51 (d,  $J$  = 1.6 Hz, 1H), 8.26 (d,  $J$  = 8.4 Hz, 1H), 7.74 (d,  $J$  = 2.1 Hz, 1H), 7.72 (t,  $J$  = 1.2 Hz, 1H), 7.65 (d,  $J$  = 8.2 Hz, 1H), 7.61 (dd,  $J$  = 7.0, 1.9 Hz, 1H), 7.52 (dd,  $J$  = 8.2, 2.1 Hz, 1H), 7.43 (m, 1H), 7.39 – 7.32 (m, 3H), 6.29 (t,  $J$  = 6.8 Hz, 1H), 4.56 (d,  $J$  = 6.3 Hz, 2H), 2.08 (s, 3H).  $^{13}C$  NMR (100 MHz, DMSO- $d_6$ )  $\delta$ : 162.98, 162.12, 149.92, 149.43, 141.81, 141.53, 139.92, 138.56, 138.10, 136.81, 136.52, 132.48, 131.98, 129.60, 128.75, 126.50, 124.40, 122.70, 121.83, 121.51, 111.77, 105.98, 41.61, 17.46. HRMS-EI  $m/z$   $[M+H]^+$  calcd for  $C_{26}H_{21}ClN_5O_2$ : 470.1306, found: 470.1378.

**6-(2-Chloro-4-(3-methyl-2-oxopyridin-1(2H)-yl)phenyl)-N-(2-(pyridin-4-yl)ethyl)-1H-indazole-3-carboxamide (30m)** The preparation of compound **30m** was similar with that of compound **30a** to afford title compound as a white solid. Yield: 62%. mp: 138-142 °C.  $R_f$ : 0.26 (DCM/MeOH, 50/1, v/v).  $^1H$  NMR (300 MHz, DMSO- $d_6$ )  $\delta$ : 13.78 (s, 1H), 8.60 (t,  $J$  = 5.9 Hz, 1H), 8.49 (d,  $J$  = 1.7 Hz, 1H), 8.48 (d,  $J$  = 1.7 Hz, 1H), 8.26 (d,  $J$  = 8.4 Hz, 1H), 7.74 (d,  $J$  = 2.1 Hz, 1H), 7.69 (t,  $J$  = 1.2 Hz, 1H), 7.64 (d,  $J$  = 8.2 Hz, 1H), 7.61 (dd,  $J$  = 6.7, 1.9 Hz, 1H), 7.52 (dd,  $J$  = 8.2, 2.2 Hz, 1H), 7.43 (m, 1H), 7.36 – 7.33 (m, 1H), 7.32 (d,  $J$  = 1.8 Hz, 2H), 7.31 (d,  $J$  = 1.7 Hz, 1H), 6.29 (t,  $J$  = 6.8 Hz, 1H), 3.69 – 3.57 (m, 2H), 2.96 (t,  $J$  = 7.2 Hz, 2H), 2.08 (s, 3H).  $^{13}C$  NMR (100 MHz, DMSO- $d_6$ )  $\delta$ : 162.64, 162.13, 149.94, 148.98, 141.79, 141.47, 139.94, 138.83, 138.10, 136.75, 136.50, 132.47, 131.98, 129.61, 128.74, 126.49, 124.73, 124.27, 121.91, 121.43, 111.69, 105.99, 39.25, 34.86, 17.45. HRMS-EI  $m/z$   $[M+H]^+$  calcd for  $C_{27}H_{23}ClN_5O_2$ : 484.1462, found: 484.1535.

**6-(2-Chloro-4-(3-methyl-2-oxopyridin-1(2H)-yl)phenyl)-N-(2-methyltetrahydro-2H-pyran-4-yl)-1H-indazole-3-carboxamide (30n)** The preparation of compound **30n** was similar with that of compound **22a** to afford title compound as a white solid. Yield: 61%. mp: 284-289 °C. R<sub>f</sub>: 0.28 (DCM/MeOH, 50/1, v/v). <sup>1</sup>H NMR (300 MHz, DMSO-*d*<sub>6</sub>) δ: 13.78 (s, 1H), 8.37 (d, *J* = 8.3 Hz, 1H), 8.27 (dd, *J* = 8.4, 0.8 Hz, 1H), 7.74 (d, *J* = 2.1 Hz, 1H), 7.69 (t, *J* = 1.1 Hz, 1H), 7.64 (d, *J* = 8.2 Hz, 1H), 7.62 – 7.58 (m, 1H), 7.51 (dd, *J* = 8.2, 2.1 Hz, 1H), 7.46 – 7.40 (m, 1H), 7.34 (dd, *J* = 8.4, 1.4 Hz, 1H), 6.29 (t, *J* = 6.8 Hz, 1H), 4.11 (m, 1H), 3.95 – 3.86 (m, 2H), 3.47 – 3.40 (m, 2H), 2.08 (s, 3H), 1.82 – 1.63 (m, 4H). <sup>13</sup>C NMR (100 MHz, DMSO-*d*<sub>6</sub>) δ: 162.12, 161.87, 141.79, 141.47, 139.95, 138.98, 138.13, 136.73, 136.55, 132.49, 131.98, 129.59, 128.76, 126.52, 124.25, 121.95, 121.52, 111.66, 105.98, 66.79, 45.48, 32.89, 17.48. HRMS-EI *m/z* [M+H]<sup>+</sup> calcd for C<sub>25</sub>H<sub>24</sub>ClN<sub>4</sub>O<sub>3</sub>: 463.1459, found: 463.1532.

**6-(2-Chloro-4-(3-methyl-2-oxopyridin-1(2H)-yl)phenyl)-N-(1-methylpiperidin-4-yl)-1H-indazole-3-carboxamide (30o)** The preparation of compound **30o** was similar with that of compound **30a** to afford title compound as a white solid. Yield: 54%. mp: 277-282 °C. R<sub>f</sub>: 0.14 (DCM/MeOH, 50/1, v/v). <sup>1</sup>H NMR (300 MHz, DMSO-*d*<sub>6</sub>) δ: 13.75 (s, 1H), 8.26 (d, *J* = 4.4 Hz, 1H), 8.24 (d, *J* = 4.4 Hz, 1H), 7.74 (d, *J* = 2.1 Hz, 1H), 7.68 (s, 1H), 7.64 (d, *J* = 8.3 Hz, 1H), 7.60 (m, 1H), 7.51 (dd, *J* = 8.2, 2.2 Hz, 1H), 7.43 (m, 1H), 7.33 (dd, *J* = 8.4, 1.4 Hz, 1H), 6.29 (t, *J* = 6.8 Hz, 1H), 3.84 (m, 1H), 2.82 (m, 2H), 2.21 (s, 3H), 2.07 (s, 3H), 2.03 (m, 2H), 1.75 (m, 4H). <sup>13</sup>C NMR (100 MHz, DMSO-*d*<sub>6</sub>) δ: 162.14, 161.99, 141.76, 141.48, 139.95, 138.94, 138.16, 136.70, 136.54, 132.49, 131.96, 129.58, 128.74, 126.51, 124.21, 121.93, 121.47, 111.69, 106.03, 54.85, 46.18, 46.01, 31.65, 17.48. HRMS-EI *m/z* [M+H]<sup>+</sup> calcd for C<sub>26</sub>H<sub>27</sub>ClN<sub>5</sub>O<sub>2</sub>: 476.1775, found: 476.1848.

**6-(2-Chloro-4-(3-methyl-2-oxopyridin-1(2H)-yl)phenyl)-N-((tetrahydro-2H-pyran-4-yl)methyl)-1H-indazole-3-carboxamide (30p)** The preparation of compound **30p** was similar with that of compound **22a** to afford title compound as a white solid. Yield: 51%. mp: 258-262 °C. R<sub>f</sub>: 0.29 (DCM/MeOH, 50/1, v/v). <sup>1</sup>H NMR (300 MHz, DMSO-*d*<sub>6</sub>) δ: 13.77 (s, 1H), 8.49 (t, *J* = 6.2 Hz, 1H), 8.26 (q, *J* = 6.7 Hz, 1H), 7.70 (m, 2H), 7.61 (m, 2H), 7.54 – 7.46 (m, 1H), 7.42 (s, 1H), 7.32 (q, *J* = 6.0 Hz, 1H), 6.28 (t, *J* = 6.1 Hz, 1H), 3.86 (m, 2H), 3.33 – 3.17 (m, 4H), 2.07 (m, 3H), 1.88 (m, 1H), 1.60 (m, 2H), 1.35 – 1.06 (m, 2H). <sup>13</sup>C NMR (100 MHz, DMSO-*d*<sub>6</sub>) δ: 162.73, 162.12, 141.78, 141.47, 139.95, 138.97, 138.13, 136.72, 136.55, 132.49, 131.97, 129.59, 128.76, 126.52, 124.23, 121.97, 121.45, 111.65, 105.99, 67.26, 44.53, 35.49, 31.03, 17.48. HRMS-EI *m/z* [M+H]<sup>+</sup> calcd for C<sub>26</sub>H<sub>26</sub>ClN<sub>4</sub>O<sub>3</sub>: 477.1615, found: 477.1688.

**6-(2-Chloro-4-(3-methyl-2-oxopyridin-1(2H)-yl)phenyl)-N-((1-methylpiperidin-4-yl)methyl)-1H-indazole-3-carboxamide (30q)** The preparation of compound **30q** was similar with that of compound **30a** to afford title compound as a white solid. Yield: 53%. mp: 168-173 °C. R<sub>f</sub>: 0.15 (DCM/MeOH, 50/1, v/v). <sup>1</sup>H NMR (300 MHz, DMSO-*d*<sub>6</sub>) δ: 13.84 (s, 1H), 8.56 (t, *J* = 6.1 Hz,

1H), 8.30 (d,  $J = 8.5$  Hz, 1H), 7.79 (d,  $J = 2.1$  Hz, 1H), 7.74 (d,  $J = 1.1$  Hz, 1H), 7.69 (d,  $J = 8.3$  Hz, 1H), 7.68 (m, 1H), 7.56 (dd,  $J = 8.2, 2.1$  Hz, 1H), 7.49 (m, 1H), 7.38 (dd,  $J = 8.4, 1.4$  Hz, 1H), 6.35 (t,  $J = 6.8$  Hz, 1H), 3.28 (t,  $J = 6.3$  Hz, 2H), 2.96 (m, 2H), 2.33 (s, 3H), 2.12 (m, 5H), 1.72 (m, 3H), 1.43 – 1.24 (m, 2H).  $^{13}\text{C}$  NMR (100 MHz, DMSO- $d_6$ )  $\delta$ : 162.70, 162.12, 141.79, 141.48, 139.96, 138.91, 138.16, 136.71, 136.56, 132.49, 131.96, 129.59, 128.76, 126.53, 124.21, 121.94, 121.44, 111.68, 105.98, 54.99, 45.79, 44.09, 35.26, 29.45, 17.48. HRMS-EI  $m/z$   $[\text{M}+\text{H}]^+$  calcd for  $\text{C}_{27}\text{H}_{29}\text{ClN}_5\text{O}_2$ : 490.1932, found: 490.2004.

**5.2. In vitro PAK Enzyme Assay.** Inhibitory effect of compounds against kinases activity were determined as previously reported [37]. Generally, the tests were performed at Reaction Biology Corporation using the “HotSpot” assay platform. The kinase and corresponding substrate were mixed with the reaction buffer (20 mM Hepes pH 7.5, 10 mM  $\text{MgCl}_2$ , 1 mM EGTA, 0.02% Brij35, 0.02 mg/mL BSA, 0.1 mM  $\text{Na}_3\text{VO}_4$ , 2 mM DTT, 1% DMSO) at room temperature. Then DMSO solution of compound (starting at 10  $\mu\text{M}$  with 3-fold serial dilution) were added into the kinase reaction mixture at room temperature. After 20 min, the reaction was initiated by addition of a mixture of ATP (Sigma) and  $^{33}\text{P}$  ATP (PerkinElmer) to a final concentration of 10  $\mu\text{M}$ , followed by the incubation of 120 min at 25  $^\circ\text{C}$ . The kinase activities were detected by filter-binding method. Kinase activity data of test sample were expressed as the percent remaining kinase activity compared to vehicle (DMSO) reactions.

**5.3. Antiproliferative activity Assay.** The human cancer cell lines were purchased from the American Type Culture Collection (ATCC, Manassas, VA, USA). The cell lines (MDA-MB-231, HCT-116) were maintained in culture media at 37  $^\circ\text{C}$  with 5%  $\text{CO}_2$ . Cells were plated in 96-well culture plates (4000/well). Cell proliferation was determined after treatment with compounds for 72 h. Cell viability was measured by Cell Titer-Glo assay (Promega, USA) following manufacturer’s instructions, and luminescence was measured in a multilabel reader (Envision2014, PerkinElmer, USA).

**5.4. Wound Healing Assay.** For the wound healing assay, MDA-MB-231 or HCT-116 cells were cultured to confluence in six-well plates and wounded using a sterilized pipet tip to make a straight scratch. The wounded cell monolayers were washed three times with phosphate-buffered saline (PBS) and incubated in serum-free medium. Then cells were treated with compound **301** with different concentrations followed by at 24 h incubation and photographed at 24 with an inverted microscope.

**5.5. Transwell invasion Assays.** Invasion assays were performed using modified Boyden chambers with a polycarbonate nucleopore membrane. Matrigel was pre-coated on the bottom. Then,  $1 \times 10^5$  MDA-MB-231 or HCT-116 cells in 100 mL serum-free DMEM supplemented with 0.1% bovine serum were placed in the upper part of each chamber and the lower compartments

were filled with DMEM containing 10% FBS. After incubation for 24 h at 37 °C, the non-invaded cells were removed from the upper surface of the filter with a cotton swab, and the invaded cells on the lower surface of the filter were fixed, stained, photographed, and counted under high-power magnification.

**5.6. Western Blotting.** To determine the expression of protein, whole cell extracts were prepared from  $1 \times 10^6$  cells in RIPA lysis buffer (50 mM Tris/HCl pH 7.4, 150 mM NaCl, 1% Nonidet P-40, 0.25% Na-deoxycholate, 1 mM EDTA and protease inhibitor cocktail). Equal amounts of denatured protein were separated by SDS-PAGE and transferred to a PVDF membrane (Millipore). The membrane was blocked with 5% nonfat dry milk in TBS-T (20 mM Tris, pH 7.4, 137 mM NaCl, 0.05% Tween-20) for 1 h at room temperature, and the proteins were probed with antibodies specific to PAK1, phospho-PAK1/Ser<sup>144</sup>, Snail and Actin. All PVDF membranes were detected by chemiluminescence (ECL, Pierce Technology).

**5.7. Molecular Modeling Study.** The protein was prepared the Protein Preparation Wizard workflow in Schrödinger 2009 platform (Schrödinger, LLC, New York, NY). Docking was performed into the predefined kinase ATP-binding pocket. Hydrogens were added to the modelled PAK1 kinase domain (PDB code 5DEY) and PAK4 kinase domain (PDB code 5XVA). The ligand was placed in the kinase ATP-binding pocket and aligned manually to avoid atom clashes. The docked poses were evaluated and ranked by default Glide score. Each docking experiment was performed 10 times, yielding 10 docked conformations. The solutions were ranked by the calculated binding free energy. Figures were shown using PyMOL. MD simulations were performed using AMBER 18 software package [38]. The PAK1 and PAK4-compound 301 systems were solvated in a truncated octahedral box of TIP3P water and neutralized with sodium or chlorine ions. Protein and ligand were charged with amber ff99SB and gaff force fields, respectively. Energy minimization was conducted with a force constraint of 500 kcal/mol prior to MD. Heating simulation was performed from 0 to 300 K using the langevin thermostat with a collision rate of 5 ps<sup>-1</sup>, and a total of 5 ns heating simulation was accomplished in NVT ensemble with a time step of 2 fs. Equilibrium MD simulations 50 ns were implemented for protein-ligand systems, respectively, in which NPT ensemble was employed with a time step of 2 fs. The Cpptraj module was used to analyze the generated trajectory. The binding free energy of ligand was calculated using MM-GB/SA algorithm [39] based on the snapshots extracted from the trajectory of 30-50 ns with an interval of 2 ps, and the binding free energy was decomposed on per residues of PAK1 and PAK4, both of which were conducted with Amber package.

### 5.8. Statistical analyses

Statistical analyses were calculated using a one-way ANOVA. For all the tests, only a P value < 0.05 was considered statistically significant. All the descriptive data are reported as the mean ±

SD. GraphPad Prism and SPSS software were used for the statistical analyses.

#### Authors' contribution

LT, CYD, ZML and LHM designed the study. ZML, FXB and WC performed all the experiments. LHM assisted in biological assays. ZML, LHM and LS analyzed the data. WM, ZL and ZYM participated in interpretation of results. ZML, LHM and LS wrote the manuscript. All authors read and approved the manuscript.

#### AUTHOR INFORMATION

##### Corresponding Authors

\*(Hongmei Li) Tel: +86-25-86185163; Fax: +86-25-86185155; E-mail: lihongmei@cpu.edu.cn

\*(Tao Lu) Tel: +86-25-86185163; Fax: +86-25-86185155; E-mail: lutao@cpu.edu.cn

\*(Yadong Chen) Tel: +86-25-86185163; Fax: +86-25-86185155; E-mail: ydchen@cpu.edu.cn

#### NOTES

The authors declare that they have no known competing financial interests or personal relationships that could have appeared to influence the work reported in this paper.

#### ABBREVIATIONS

**PAK1**, p21-activated kinase 1; **ATP**, Adenosine triphosphate; **hERG**, human Ether-a-go-go Related Gene; **PDB**, Protein Data Bank; **EMT**, epithelial mesenchymal transition; **IC<sub>50</sub>**, Inhibitory concentration 50; **SD**, standard deviation; **MD**, molecular dynamics; **SAR**, structure-activity relationship; **RMSD**, root-mean-square deviation; **NMR**, nuclear magnetic resonance; **DMSO**, Dimethyl sulfoxide; **DHP**, 3,4-Dihydro-2H-Pyran; **ACN**, Acetonitrile; **TLC**, thin-layer chromatography; **DIEA**, N,N-Diisopropylethylamine; **DMF**, dimethylformamide; **HATU**, O-(7-Azabenzotriazol-1-yl)-N,N,N',N'-tetramethyluronium hexafluorophosphate; **PAINS**, pan assay interference compounds; **NMR**, nuclear magnetic resonance.

#### ACKNOWLEDGMENT

This research was supported by grants from the National Natural Science Foundation of China (81502925, 81973188 and 81803033), Jiangsu Province Natural Science Funds for Young Scholar (BK20180573), "Double First-Class University project" (CPU2018GF02), China Postdoctoral Science Foundation (2018M632428) and College Students Innovation Project for the R&D of Novel Drugs (J1310032).

## References:

- [1]. M. Radu, G. Semenova, R. Kosoff, J. Chernoff, PAK signalling during the development and progression of cancer, *Nat. Rev. Cancer*. 14 (2014) 13-25.
- [2]. C.C. Ong, S. Gierke, C. Pitt, M. Sagolla, C.K. Cheng, W. Zhou, A.M. Jubb, L. Strickland, M. Schmidt, S.G. Duron, D.A. Campbell, W. Zheng, S. Dehdashti, M. Shen, N. Yang, M.L. Behnke, W. Huang, J.C. McKew, J. Chernoff, W.F. Forrest, P.M. Haverty, S.F. Chin, E.A. Rakha, A.R. Green, I.O. Ellis, C. Caldas, T.O Brien, L.S. Friedman, H. Koeppen, J. Rudolph, K.P. Hoeflich, Small molecule inhibition of group I p21-activated kinases in breast cancer induces apoptosis and potentiates the activity of microtubule stabilizing agents, *Breast. Cancer. Res.* 17 (2015) 59.
- [3]. J. Rudolph, J.J. Crawford, K.P. Hoeflich, W. Wang, Inhibitors of p21-activated kinases (PAKs), *J. Med. Chem.* 58 (2015) 111-129.
- [4]. E.R. Zynda, M.H. Maloy, E.S. Kandel, The role of PAK1 in the sensitivity of kidney epithelial cells to ischemia-like conditions, *Cell. Cycle*. 2019 5 (2019) 596-604.
- [5]. M.N. Zhan, X.T. Yu, J. Tang, C.X. Zhou, C.L. Wang, Q.Q. Yin, X.F. Gong, M. He, J.R. He, G.Q. Chen, Q. Zhao, MicroRNA-494 inhibits breast cancer progression by directly targeting PAK1, *Cell. Death. Dis.* 8 (2017) 2529.
- [6]. C.C. Ong, A.M. Jubb, P.M. Haverty, W. Zhou, V. Tran, T. Truong, H. Turley, T. O' Brien, D. Vucic, A.L. Harris, M. Belvin, L.S. Friedman, E.M. Blackwood, H. Koeppen, K.P. Hoeflich, Targeting p21-activated kinase 1 (PAK1) to induce apoptosis of tumor cells, *Proc. Natl. Acad. Sci. U. S. A.* 17 (2011) 7177-7182.
- [7]. D. Guo, Y. Tan, D. Wang, K.S. Madhusoodanan, Y. Zheng, T. Maack, J.J. Zhang, and X. Huang, A Rac-cGMP Signaling Pathway, *Cell*. 128 (2007) 341-355.
- [8]. H. Lu, S. Liu, G. Zhang, W. Bin, Y. Zhu, D.T. Frederick, Y. Hu, W. Zhong, S. Randell, N. Sadek, W. Zhang, G. Chen, C. Cheng, J. Zeng, L.W. Wu, J. Zhang, X. Liu, W. Xu, C. Krepler, K. Sproesser, M. Xiao, B. Miao, J. Liu, C.D. Song, J.Y. Liu, G.C. Karakousis, L.M. Schuchter, Y. Lu, G. Mills, Y. Cong, J. Chernoff, J. Guo, G.M. Boland, R.J. Sullivan, Z. Wei, J. Field, R.K. Amaravadi, K.T. Flaherty, M. Herlyn, X. Xu, W. Guo, PAK signalling drives acquired drug resistance to MAPK inhibitors in BRAF-mutant melanomas, *Nature*. 550 (2017) 133-136.
- [9]. L. Chen, S.N. Bi, J.Z. Zhou, C.J. Wang, S.Q. Xie, Targeting p21-activated kinase 1 inhibits growth and metastasis via Raf1/MEK1/ERK signaling in esophageal squamous cell carcinoma cells, *Cell. Commun. Signal.* 17 (2019) 31-48.
- [10]. H.Y. Chow, B. Dong, C.A. Valencia, C.T. Zeng, J.N. Koch, T.Y. Prudnikova, J. Chernoff, Group I Paks are essential for epithelial-mesenchymal transition in an Apc-driven model of colorectal cancer, *Nat. Commun.* 9 (2018) 3473.
- [11]. Z. Lv, M. Hu, J. Zhen, J. Lin, Q. Wang, R. Wang, Rac1/PAK1 signaling promotes epithelial mesenchymal transition of podocytes in vitro via triggering betacatenin transcriptional activity under high glucose conditions, *Int. J. Biochem. Cell. B.* 45 (2013) 255-264.
- [12]. V.D. Delorme-Walker, J.R. Peterson, J. Chernoff, C.M. Waterman, G. Danuser, C. Der-Mardirossian, Pak1 regulates focal adhesion strength, myosin IIA distribution, and actin dynamics to optimize cell migration, *J. Cell. Biol.* 193 (2011) 1289-1303.
- [13]. Y.X. Ye, Y.H. Zhou, Q. Zheng, S.S. Tang, Y. Dai, Y. Zhou, M.J. Wang, J. Zhou, X.J. Lu, L.L. Wang, B.W. Ying, Pak1 gene functioned differentially in different BCR-ABL subtypes in leukemia genesis and treatment response through STAT5 pathway, *Leukemia. Res.* 79 (2019) 6-16.

- [14]. W. Senapedis, M. Crochiere, E. Baloglu, Y. Landesman, Therapeutic potential of targeting PAK signaling, anti-cancer agents, *Med. Chem.* 16 (2015) 75-88.
- [15]. B.W. Murray, C. Guo, J. Piraino, J.K. Westwick, C. Zhang, J. Lamerdin, E. Dagostino, D. Knighton, C. Loi, M. Zager, E. Kraynov, I. Popoff, J.G. Christensen, R. Martinez, S.E. Kephart, J. Marakovits, S. Karlicek, S. Bergqvist, T. Smeal, Small-molecule p21-activated kinase inhibitor PF-3758309 is a potent inhibitor of oncogenic signaling and tumor growth, *Proc. Natl. Acad. Sci. U. S. A.* 107 (2010) 9446-9451.
- [16]. J.C. James, L. Wendy, A. Ignacio, Structure-guided design of group I selective p21-activated kinase inhibitors, *J. Med. Chem.* 58 (2015) 5121-5136.
- [17]. A.S. Karpov, P. Amiri, C. Bellamacina, M.H. Bellance, W. Breitenstein, D. Daniel, R. Denay, D. Fabbro, C. Fernandez, I. Galuba, S. Guerro-Lagasse, S. Gutmann, L. Hinh, W. Jahnke, J. Klopp, A. Lai, M.K. Lindvall, S. Ma, H. Mobitz, S. Pecchi, G. Rummel, K. Shoemaker, J. Trappe, C. Voliva, S.W. Cowan-Jacob, A.L. Marzinzik, Optimization of a dibenzodiazepine hit to a potent and selective allosteric PAK1 inhibitor, *ACS Med. Chem. Lett.* 6 (2015) 776-781.
- [18]. W. McCoull, E.J. Hennessy, K. Blades, C. Chuaqui, J.E. Dowling, A.D. Ferguson, F.W. Goldberg, N. Howe, C.R. Jones, P.D. Kemmitt, G. Lamont, J.G. Varnes, R.A. Ward, and B. Yang, Optimization of Highly Kinase Selective Bis-anilino Pyrimidine PAK1 Inhibitors, *ACS Med. Chem. Lett.* 7 (2016) 1118-1123.
- [19]. J. Rudolph, I. Aliagas, J.J. Crawford, S. Mathieu, W. Lee, Q. Chao, P. Dong, L. Rouge, W. Wang, C. Heise, L.J. Murray, H. La, Y. Liu, G. Manning, F. Diederich, and K.P. Hoeflich, Leveraging the Pre-DFG Residue Thr-406 To Obtain High Kinase Selectivity in an Aminopyrazole-Type PAK1 Inhibitor Series, *ACS Med. Chem. Lett.* 6 (2015) 711-715.
- [20]. C.O. Ndubaku, J.J. Crawford, J. Drobnick, I. Aliagas, D. Campbell, P. Dong, L.M. Dorman, S. Duron, J. Epler, L. Gazzard, C.E. Heise, K.P. Hoeflich, D. Jakubiak, H. La, W. Lee, B. Lin, J.P. Lyssikatos, J. Maksimoska, R. Marmorstein, L.J. Murray, T.O Brien, A. Oh, S. Ramaswamy, W. Wang, X. Zhao, Y. Zhong, E. Blackwood, J. Rudolph, Design of selective PAK1 inhibitor G-5555: improving properties by employing an unorthodox low-pK a polar moiety, *ACS Med. Chem. Lett.* 6 (2015) 1241-1246.
- [21]. J. Rudolph, L.J. Murray, C.O. Ndubaku, Chemically diverse Group I p21-activated kinase (PAK) inhibitors impart acute cardiovascular toxicity with a narrow therapeutic window, *J. Med. Chem.* 59 (2016) 5520-5541.
- [22]. S. Angapelly, P.V. Sri Ramya, A. Angeli, C.T. Supuran, M. Arifuddin, Sulfocoumarin, coumarin, 4-sulfamoylphenyl-bearing indazole-3-carboxamide hybrids: synthesis and selective inhibition of tumor-associated carbonic anhydrase isozymes IX and XII, *Chem. Med. Chem.* 19 (2017) 1578-1584.
- [23]. S. Tomassi, J. Lategahn, J. Engel, M. Keul, H.L. Tumbrink, J. Ketzer, T. Mühlenberg, M. Baumann, C. Schultz-Fademrecht, S. Bauer, D. Rauh, Indazole-based covalent inhibitors to target drug-resistant epidermal growth factor receptor, *J. Med. Chem.* 60 (2017) 2361-2372.
- [24]. P. Li, H.F. Zhou, F. Liu, Z.X. Hu, H.X. Wang, Synthesis of [2-(2-oxazolonyl)-6-(2-pyridyl)] phenylpalladium(II) chloride and its catalytic activity in Suzuki coupling, *Inorg. Chem. Commun.* 32 (2013) 78-81.
- [25]. L. Rooney, A. Vidal, N. Devereux, D.C. Tully, Discovery, optimization and biological evaluation of 5-(2-(trifluoromethyl)phenyl)indazoles as a novel class of transient receptor potential A1 (TRPA1) antagonists, *J. Med. Chem.* 57 (2014) 5129-5140.

- [26]. E.X. Zhang, J.Z. Tang, S.H. Li, P. Wu, J.E. Moses, K. B. Sharpless, Chemoselective synthesis of polysubstituted pyridines from heteroaryl fluorosulfates, *Chem-Eur. J* 22 (2016) 5692-5697.
- [27]. C.S. Li, D.D. Dixon, An efficient copper-catalyzed coupling reaction of pyridin-2-ones with aryl and heterocyclic halides based on Buchwald's protocol, *Tetrahedron*. 61 (2005) 2931-2939.
- [28]. T. Liang, C. Chen, Side-arm control in phosphine-sulfonate palladium- and nickel-catalyzed ethylene polymerization and copolymerization, *Organometallics*. 36 (2017) 2338-2344.
- [29]. Y.H. Wang, W. Cai, Y.B. Cheng, X.C. Lin, Discovery of Biaryl Amides as Potent, Orally Bioavailable and CNS Penetrant ROR $\gamma$ t Inhibitors, *ACS Med. Chem. Lett.* 6 (2015) 787-792.
- [30]. W. McCoull, E.J. Hennessy, K. Blades, M.R. Box, C. Chuaqui, J.E. Dowling, C.D. Davies, A.D. Ferguson, F.W. Goldberg, N.J. Howe, P.D. Kemmitt, G.M. Lamont, K. Madden, C. McWhirter, J.G. Varnes, R.A. Ward, J.D. Williams, B. Yang, Identification and optimisation of 7-azaindole PAK1 inhibitors with improved potency and kinase selectivity, *Med. Chem. Commun.* 5 (2014) 1533-1539.
- [31]. J.J. Crawford, W. Lee, I. Aliagas, S. Mathieu, K.P. Hoeflich, W. Zhou, W. Wang, L. Rouge, L. Murray, H. La, N. Liu, P.W. Fan, J. Cheong, C.E. Heise, S. Ramaswamy, R. Mintzer, Y. Liu, Q. Chao, J. Rudolph, Structure-guided design of group I selective p21-activated kinase inhibitors, *J. Med. Chem.* 58 (2015) 5121-5136.
- [32]. C.Z. Hao, F. Zhao, H.Y. Song, J. Guo, X.D. Li, X.L. Jiang, R. Huan, S. Song, Q.L. Zhang, R.F. Wang, K. Wang, Y. Pang, T.C. Liu, T.Q. Lu, J. Wang, B. Lin, Z.G. He, H.T. Li, F. Li, D.M. Zhao, M.S. Cheng, Structure-based design of 6-chloro-4-aminoquinazoline-2-carboxamide derivatives as potent and selective p21-activated Kinase 4 (PAK4) inhibitors, *J. Med. Chem* 61 (2017) 265-285.
- [33]. L.E. Arias-Romero, J. Chernoff, A tale of two Paks, *Mol. Biol. Cell*. 100 (2008) 97.
- [34]. A. Minden, PAK4-6 in cancer and neuronal development, *Cell. Logist.* 2 (2012) 95-104.
- [35]. A. Whale, F.N. Hashim, S. Fram, G.E. Jones, C.M. Wells, Signaling to cancer cell invasion through PAK family kinases, *Front. Biosci.* 16 (2011) 849-864.
- [36]. Z. Yang, S. Rayala, D. Nguyen, R.K. Vadlamudi, S. Chen, R. Kumar, Pak1 phosphorylation of snail, a master regulator of epithelial-to-mesenchyme transition, modulates snail's subcellular localization and functions, *Cancer research*. 65 (2005) 3179-3184.
- [37]. W. Yang, Y. Chen, X. Zhou, Y. Gu, W. Qian, F. Zhang, W. Han, T. Lu, W. Tang, Design, synthesis and biological evaluation of bis-aryl ureas and amides based on 2-amino-3-purinylypyridine scaffold as DFG-out B-Raf kinase inhibitors, *Eur. J. Med. Chem.* 89 (2015) 581-596.
- [38]. D.A. Case, T.E. Cheatham, T. Darden, H. Gohlke, R. Luo, K.M. Merz, A. Onufriev, C. Simmerling, B. Wang, R.J. Woods, The Amber biomolecular simulation programs, *J. Comput. Chem.* 26 (2005) 1668-1688.
- [39]. T. Hou, J. Wang, Y. Li, W. Wang, Assessing the performance of the MM/PBSA and MM/GBSA methods. 1. The accuracy of binding free energy calculations based on molecular dynamics simulations, *J. Chem. Inf. Model.* 51 (2011) 69-82.

**Highlight**

1. *1H*-indazole-3-carboxamide scaffold were identified as PAK1 inhibitors by virtual screening.
2. Substituted hydrophobic ring of **301** in the deep back pocket achieved selective binding towards the PAK subtype.
3. **301** dose-dependently suppressed the migration and invasion of PAK1-related tumour cells.

Journal Pre-proof

**Declaration of interests**

The authors declare that they have no known competing financial interests or personal relationships that could have appeared to influence the work reported in this paper.

The authors declare the following financial interests/personal relationships which may be considered as potential competing interests:

Journal Pre-proof